

Development of Silicon-based microfluidic platform for flow cytometry



NanoSYD, SDU Sønderborg
Supervisor: Jakob Kjelstrup-Hansen

Submission date 02-06-2009
Examination date 15-06-2009
Mechatronics – 5MC – SPRO8

Bjarke Harbo Jacobsen

Preface

This report is composed as part of the Mechatronics final exam project (30 ETCS points). It is written for NanoSYD at the University of Southern Denmark, Sønderborg.

The final conclusion of the project will be placed right after the project statement. This is done so that people interested in my work, can get a quick overview of the associated problems and the conclusions developed, without having to go through all the documentation.

It has been a large project, with work needed done in several areas. My part has mostly been about creating the silicon-based hydrodynamic flow systems, which I got acquainted with last semester. Also a big part this year has been trying to seal, test and then comparing the systems to a commercial system, and to similar system created by my fellow student Stefan Johansen.

During the project there has been a lot of collaboration with Stefan, and especially with the parts where our projects have been overlapping. There has been a lot of work to do, during our study time, where we have supported each other also. So a great thanks to you for helping me keep up the spirit and pushing forward.

I would also like to thank my supervisor, Jakob Kjelstrup-Hansen, for all the help. I have had many supervisors through the last five years, but only few who are as engaged and helpful. He has had many ideas and suggestions, and is usually able to explain things to me so that I understand them right.

Also I would like to thank Casper Kunstmann-Olsen, for letting me use the Navitar setup he is currently working on (even when I do not want to give it back) and also for giving a helping hand now and then.

And lastly a thanks to all those that has been helping me in general or helped create a nice working atmosphere, Ralph, Manuela and the rest of you which are also working in the same laboratories.

Sønderborg 2.6.2009

Bjarke H. Jacobsen
University of Southern Denmark, Sønderborg



Table of contents

Preface	2
Table of contents	3
Introduction	5
1.1 Project statement	5
1.1.1 Project background.....	5
1.1.2 Problem statement	6
1.1.3 Problem limitation.....	7
1.1.4 Project conclusion.....	8
1.2 Flow cytometry	10
1.2.1 Hydrodynamic focusing	10
1.2.2 Detection of particles.....	12
1.2.3 Sorting of particles.....	12
Techniques and materials for fabrication and characterization of the microfluidic system	13
2.1 Plasma etching	13
2.1.1 DC Sputter Deposition	15
2.1.2 RF Sputter Deposition.....	17
2.1.3 Reactive Ion Etch (RIE)	17
2.1.4 Inductively Coupled Plasma Reactive Ion Etch (ICP RIE).....	18
2.1.5 Bosch Process.....	19
2.1.6 Error minimization.....	19
2.2 Test platform	20
2.2.1 Platform base	20
2.2.2 Sealing.....	21
2.2.3 Connectors	22
2.2.4 Syringe pumps.....	22
2.2.5 Dye color	23
2.3 Microscopy	24
2.3.1 Optical microscope	24
2.3.2 Navitar setup	25
2.3.3 Fluorescence microscope	26
2.3.4 Profilometer	27
2.3.5 Interference microscope	28



Realization of the microfluidic system	29
3.1 Mask design	29
3.1.1 Wafer.....	29
3.1.2 Platform design and placement	29
3.1.3 Channel structure	30
3.1.4 Alignment and cutting marks	31
3.1.5 The real mask.....	31
3.1.6 Platform fabrication process: Creating channels in a silicon wafer	32
3.1.7 Preparing wafers for the ICP RIE.....	32
3.1.8 Recipe used for etching with the ICP RIE	34
3.1.9 Etch rate for SF ₆ on silicon wafers	35
3.1.10 Structure of the microchannels etched	39
3.1.11 Stripping the wafer for photo resist	39
3.1.12 Breaking the wafer.....	39
3.1.13 Hydrophobicity of the wafer surface.....	40
3.2 Platform assembly.....	41
3.2.1 Step 1: Apply adhesive tape	41
3.2.2 Step 2: Carve holes in the sealing for connectors	42
3.2.3 Step 3: Place the connectors	42
3.2.4 Step 4: Apply cleaning vacuum	43
3.2.5 Step 5: Water test.....	43
Results and discussion from hydrodynamic focusing experiments	44
4.1 Hydrodynamic focusing	44
4.1.1 Image gathering	47
4.1.2 Calibration measurements.....	49
4.1.3 Mutual performance comparison of platforms	49
4.1.4 Navitar microscope	50
4.1.5 Fluorescence microscope	51
4.1.6 Averaging flow measurements	55
4.1.7 Platform type comparison.....	56
4.1.8 Sources of error.....	57
List of references	58
5.1 Internet	58
5.1.1 Websites	58
5.1.2 Wikipedia.org.....	58
5.2 Bibliography.....	59
5.2.1 Articles	59
5.2.2 Books and pamphlets	60



Appendix	61
6.1 My attachments	61
6.1.1 Reynolds number	61
6.1.2 Mask design 1	62
6.1.3 Preparation progress for all wafers (1-12):	63
6.2 Attachments from other sources	64
6.2.1 Drawing of commercial system	64
6.2.2 ARcare® 7815 Clear Polyester Film	65



1 Introduction

1.1 Project statement

1.1.1 Project background

A lab-on-a-chip is a small device (typically between a few mm² and a few cm²) that can perform some type of chemical or biological analysis, which would otherwise require extensive laboratory functionalities. It most often includes a system of microfluidic channels to guide small amounts of liquid, such as the sample and the reagents required to perform the analysis, and can include several microfluidic components such as valves, pumps, mixers etc. Lab-on-a-chip devices can be applied in a range of areas, such as in analysing medical samples for example for bacteria or viruses or in investigating food for bacterial contamination.

At NanoSYD, the Mads Clausen Institute, there has recently been launched a research and development project [5.1.1.2] in collaboration with the Universities of Applied Sciences in Flensburg and Kiel which aims at developing a microfluidic platform that enables fast analysis of food samples for contamination, i.e. to detect if a particular type of cell is present in the sample. This master project will be involved in the larger project, and it should focus on developing the basic microfluidic platform for flow cytometry. In flow cytometry, the liquid, cell-containing sample is focused using the principle of hydrodynamic focusing, in which two sheath flows causes the cells to become aligned like pearls on a string. This enables the analysis of individual cells one at a time.

Lab-on-a-chip systems are today already commercially available from the company Agilent [5.1.1.1]. This system, however, can only measure large eukaryotic cells and need a minimum of 2500 cells to operate. Whereas the system that is being developed by NanoSYD will be more sensitive, and amongst other include impedance analysis, giving a more flexible and detailed measurement, which will also make it possible to measure prokaryotes.



1.1.2 Problem statement

In order to get a fully functioning lab-on-a-chip device, hydrodynamic focusing is required. This can be done using various platform materials, processed in different ways. A master thesis (Microfluidic system, by Stefan Johansen) running alongside this project, focuses on creating hydrodynamic flow focusing in Poly Methyl Methacrylate (PMMA) [5.1.2.1], using a rapid prototyping Argon Fluorine laser. By comparing results of the different type of systems, it is easier to determine the best solution used, for the larger project of fast food analysis.

Hence the aim of this project is to:

- Design, fabricate and test a Silicon-based microfluidic platform, which allows a liquid sample flow to be focussed using hydrodynamic focusing.
- Investigate a sealing method capable of enclosing the liquids pumped into the microfluidic platform.
- Be able to vary the focussed flow from 1-10 μm , which is the typical cell size range, we want to be able to measure.
- Compare performance with other systems, both commercial and the parallel project using rapid prototyping in PMMA.



1.1.3 Problem limitation

The silicon-based microfluidic platform is going to be fabricated by typical top-down fabrication techniques i.e. photolithography and subsequent plasma etching. In this fabrication process, several opportunities for optimization exists, such as the type of developer and resist used, the speed, ramping and runtime with which the photo resist is spun onto a wafer and so on. Since the main assignment in this project is hydrodynamic focusing, I will use the standard materials and recipes available in the NanoSYD cleanroom.

To help getting started, a commercial cytometry system sold by microfluidic ChipShop GmbH is going to be studied during the first stages of the project (see appendix 6.1.4). This commercial platform is constructed using channels varying in size. By making my channels approximately the same size as for this commercial system, I will be able to compare it with my silicon-based platform.

My first priority will be the hydrodynamic focusing. So to avoid spending a lot of time on etching techniques, the platforms I create will have same depth all over. Channels will be fixed in width by the pattern on a mask and therefore will not change once the mask is made. As a basis for scaling the system, four different channel widths are going to be made: 25 μm , 50 μm 100 μm and 200 μm . The 100 μm wide channel is chosen to resemble the commercial system and will have my main attention. The 50 μm and 200 μm sizes correspond to half and double size of the 100 μm system. Lastly the 25 μm size is chosen because a hydrodynamic focusing of 1-10 μm is desired, and so this system may give a better image resolution. The desired structure sizes are easy achieved with UV lithography, and I will therefore use the mask aligner for lithography steps.

In order to be able to compare performances with the other hydrodynamic focusing platforms, a standardized measurement method will be made in agreement with Stefan Johansen, and it will also be used in his project.

Normally when using hydrodynamic focusing, the focus is only made in a two dimensional level, which can be viewed from the top down. This is what I intend to do in this project. However, since the channels used are all three dimensional, hydrodynamic focusing could be done in the channels cross-section. This can for instance be done either by using inlet channels from the top and bottom also to focus this way or maybe by creating a specific corner-focusing system [5.2.1.10].



1.1.4 Project conclusion

If we start with the design of the mask, then there are a lot of things that could be improved for a new design. First of all, I mostly used the two main straight platforms in the middle of the wafer. This is partly because these gave the best results (and the only ones), but I do not think the smaller channels have been tested thoroughly, to just be cast away. Maybe it is still possible to use the 50 μm channels, or maybe even the 25 μm channels, if both oxidation of the wafers and the latest sealing method is used. However, the time was short, so focus was maintained upon the 100 μm platforms.

Now, instead of having many different platforms placed on the mask, it might be better to have only two or three platforms placed in total, and then instead place a lot of straight channels with different lengths. That way it will be easier to measure how much the pressure influence our ability to pump water through the systems.

Next, when designing new platforms, it should be taken into account that pressure might matter a lot. If we can glue very strong seals, then we should also be able to have long channels, which will make the measuring in the microscopes a lot easier. However, if the current connections can not support the pressure needed to use the smaller systems, then maybe shortening the channels, or making channels in different sizes for the same system, might help. Most of these pressure tests are still missing, because we did not use the syringe pumps to measure the pressure the filter paper, mounted to the bottom of the connectors, could withstand before loosening. So to make the optimal platform design without these results, I recommend that the channel crossing is moved, so that there will be almost an equal distance from the sample input and from the output channel, to the channel crossing.

The fabrication of the silicon channels went well. The recipe fit quite well from the start, and there was neither a problem with selectivity. But in the future it might be a better idea to produce inverted wafers, which can then be used to pour on PDMS, which will then get the desired structures. The reason for this is, that even though bonding between the silicon and the lid could be made to withstand large pressures, I felt that it was kind of random whether a good bond was made or not. Also after some time being used, the tape can begin to loosen. By using PDMS platforms we could also fit a PDMS lid on top, and the by clamping or maybe oxidation of the surfaces bonding, we would have very strong system.

After the first platform was sealed properly, hydrodynamic focusing was easily achieved, even though only viewable in large scales. As it got easier to seal the systems tight, it was possible to use a fairly high flow (250 $\mu\text{L}/\text{min}$), which for my systems made the measurements almost as good as the commercial one. However, it was not achieved to make a stable focus in the scale of 1-10 μm . To be able to better distinguish focusing in this area, either a better resolution would be needed or maybe by using smaller channels, would it be possible. If smaller channels are used, then a larger percentage of the channel is allowed to be used for the sample flows, which were the cases that gave the best pictures.

If the future of this project is to detect bead-sized objects, one at a time, at a fast pace, then maybe it would be better to forget about measuring the correct width of colored water, but



instead make experiments trying to get only one bead through the channel at a time, and then when this succeeds change sizes of the bead. The beads are also very bright in the fluorescent microscopes.

Now the sealing process was a bit of a learning progress. At first we needed to learn to mount the connectors precisely, not cut them too small, and also making sure that no dirt came into the system, and by doing so blocking the channels. Then the filter paper was not strong enough, a different pore sized paper could be tried out, but otherwise sealing as much as possible with silicone afterwards, seems to create a strong system. At one point we had a flow of more than 4000 $\mu\text{L}/\text{min}$ to see if we could get the tape or silicone glued connectors to fail, but instead water started pouring out, at the hose inlets. We did not glue on hoses, because we did not have a lot available (still waiting for the shipment to arrive).

Now when comparing the three systems: Silicon, PMMA, and the commercial, then there are different pros and cons. For production issues, the commercial system is easy to buy, but delivery time and probably also expenses make this a poor solution in the long run. The silicon wafers are quick to produce in a batch production, once the mask has been bought. The rapid prototyping system, PMMA, is of course the easiest to change. However, it is not easy to determine if the correct depth has been achieved, and so the silicon channels are far more stable in production and expected results. A hindrance for the silicon systems could be that they are not transparent. The fluorescent light was enough at 50x magnification, but if more intensive light is needed at larger magnifications, it is possible to buy special objectives or using immersion oils to compensate.

A lot of graphs have been made, but frankly I would not trust any of the results too much. There have simply been too few measurements of the same systems and also of the same platform sizes, because we first had to fabricate the systems and then learn to seal them properly.

So to sum up, a lot of testing and optimizations both in, sealing, choice of materials, pressure testing, assembling and microscopy, is needed. So depending on the intended use it might be better to focus on using the bead flow.



1.2 Flow cytometry

Flow cytometry is a way of characterizing microscopic particles in a liquid and then sorting them as wanted. To get a closer look at how this is done, we can basically divide cytometry into three main areas:

- 1) Hydrodynamic focusing
- 2) Detection of particles
- 3) Sorting of particles

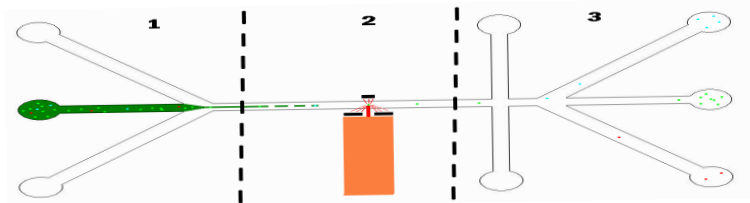


Figure 1.2: An overview of flow cytometry.

Depending on how advanced a flow cytometry is needed, further improvements can be implied in such a system, like for instance micro pumps to control the flow, or different types of measuring lights/sensors.

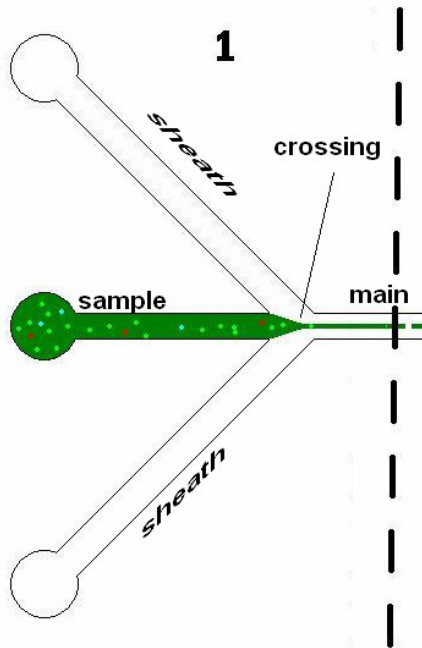


Figure 1.2.1: Hydrodynamic focusing

1.2.1 Hydrodynamic focusing

The first part of cytometry is to focus the sample flow, so that each individual particle can be detected, measured and sorted. This is done by hydrodynamic focusing. When using hydrodynamic focusing you add a sheath flow on both sides of the sample flow. Then by changing either the flow rate [$\mu\text{L}/\text{min}$] of the different flows, or by beforehand creating different channel sizes, you can control the sample flow's width in the main channel. This can only be done, because the channels used are very small. In these channels the fluid velocities are very low, resulting in a low Reynolds number (dimensionless) (see appendix 6.1.1 for calculations on my platform), which tells us whether the liquid is turbulent or laminar. Reynolds numbers below 2300 for pipes is generally considered to give a laminar flow, and thus prevents the mixing of two concurrently flowing liquids [5.1.2.5]. In fact when the Reynolds number is low enough, the only mixing that occurs is due to diffusion.

To manage the hydrodynamic focusing, a syringe pump setup is going to be used. This way the two sheath flows ratio to the sample flow can be controlled. By setting the pumps to pump a constant flow, this can be used to approximately determine the width of the focused flow, in the output channel, by assuming that the relation between the sample flow and the total output flow, is the same as the width of the focused sample flow in relation with the output width:

$$\frac{w_{ff}}{w_{output}} \approx \frac{Q_{ff}}{Q_{sample} + Q_{sheath1} + Q_{sheath2}} \Rightarrow w_{ff} \approx \frac{Q_{ff}}{Q_{sample} + Q_{sheath1} + Q_{sheath2}} \cdot w_{output} \quad (1)$$

Where generally the volumetric flow rate can be shown like this:

$$Q = \frac{V}{t} = \frac{h \cdot w \cdot l}{t} = \frac{l}{t} \cdot h \cdot w = v \cdot h \cdot w \quad \Rightarrow \quad Q = v \cdot h \cdot w \quad (2)$$

And:

Q	is the volumetric flow rate	[$\mu\text{L}/\text{min}$]
w	is the width of the channel	[μm]
V	is the volume	[μL]
t	is time	[min]
h	is the height of the channel	[μm]
l	is the distance the liquid has moved	[μm]
v	is the speed of the travelling liquid	[$\mu\text{m}/\text{min}$]

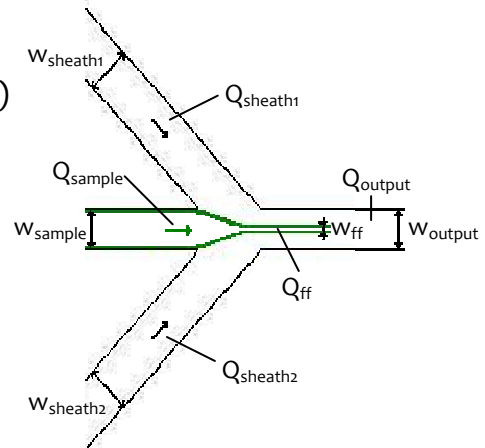


Figure 1.2.2: Detailed hydrodynamic flow focusing overview.

The above equation (1) is only approximately correct. This is due to the disregard of speed. A better approximation can be made if we assume v to be average across the channel. In reality the speed differs between the channel edges and the middle stream [5.1.1.3]. For a detailed explanation usable on square channels see [5.2.2.1]. Having made this assumption we know that what goes into the channels must come out again. This is the law of mass conservation, and we get for the sample flow, that:

$$Q_{ff} = Q_{sample} \quad \Rightarrow \quad v_{ff} \cdot h_{ff} \cdot w_{ff} = Q_{sample} \quad \Rightarrow \quad w_{ff} = \frac{Q_{sample}}{h_{ff} \cdot v_{ff}} \quad (3)$$

For the output flow we have that:

$$\begin{aligned} Q_{output} &= Q_{sample} + Q_{sheath1} + Q_{sheath2} \\ \Downarrow \\ v_{output} \cdot h_{output} \cdot w_{output} &= Q_{sample} + Q_{sheath1} + Q_{sheath2} \\ \Downarrow \\ w_{output} &= \frac{Q_{sample} + Q_{sheath1} + Q_{sheath2}}{h_{output} \cdot v_{output}} \end{aligned} \quad (4)$$

Hence the relationship by law of mass conservation can be expressed as:

$$\frac{w_{ff}}{w_{output}} = \frac{h_{output} \cdot v_{output} \cdot Q_{sample}}{h_{ff} \cdot v_{ff} \cdot (Q_{sample} + Q_{sheath1} + Q_{sheath2})} \quad (5)$$

Where:

$$h_{ff} = h_{output} = h_{sample} = h_{sheath}$$

Giving:

$$\frac{w_{ff}}{w_{output}} = \frac{v_{output}}{v_{ff}} \cdot \frac{Q_{sample}}{Q_{sample} + Q_{sheath1} + Q_{sheath2}} \quad (6)$$

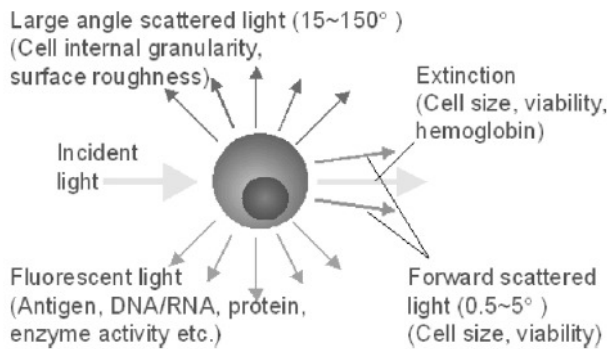


As we see the velocity for the flow in the output channel and the focused flow is needed to give a precise relation. However, even though the output speed can easily be found using (4), the focused flow speed is hard to calculate. Since I have no flow measuring devices at hand, I will therefore use equation (1) for estimating results.

This is the part of flow cytometry I shall focus on in this project.

1.2.2 Detection of particles

To detect the microscopic particles focused in the main channel, laser light is often used. This can be to get enough light intensity or to be able to look at or filter specific wavelengths. The light can be detected in different ways, and depending on the method used different information can be collected:



[5.2.1.3] Figure 1.2.4: Different measuring methods

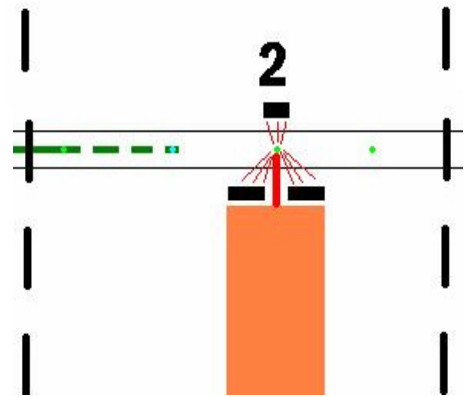


Figure 1.2.3: Detection of particles

Since I only need to be able to measure the focused channel width, I can settle with the results gathered from backscattered light, either from dye in plain white light, or from fluorescent dye excited with UV light, which can be achieved in an ordinary microscope.

1.2.3 Sorting of particles

The last step is sorting of the particles. For instance if only certain bacteria or cells need to be collected separately. This can be done in different ways. On the picture (left) is show a method where you, like hydrodynamic focusing, uses two side channels to push the focused flow to either side, by pumping extra liquid in here.

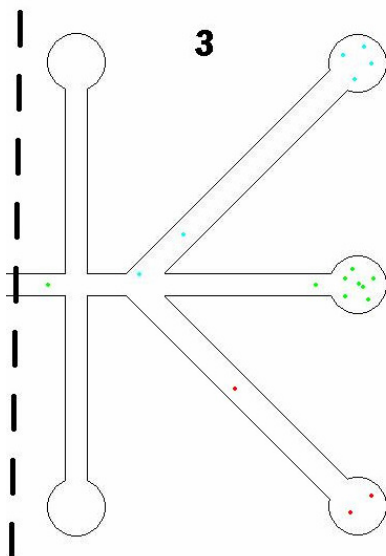
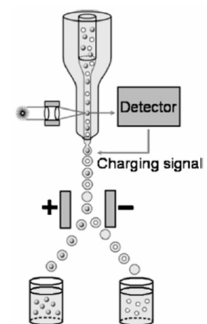


Figure 1.2.5: Sorting of particles

Another way to control the sorting is by capturing each particle in a separate drop, created by narrowing the focused flow in air [5.2.1.1]. This drop is then charged differently depending on the detected reflected fluorescent light. Then by applying an electric field the drops (still containing the particle) can be directed into the desired beholder:



[5.2.2.1]
 Figure 1.2.6:
 Fluorescence
 activated sorting

2 Techniques and materials for fabrication and characterization of the microfluidic system

2.1 Plasma etching

Silicon can be etched by Cl, F, or Br (halogens) [5.2.2.3]. To get a high anisotropy (vertical sidewalls) this is often done in a plasma enhanced process where etching occurs by a combination of physical (sputtering) and chemical (reactive) etching. In this project fluorine will be used for plasma etching, generated from available SF₆, in the following reaction:



In the plasma, different reactions happen that help the etch process [5.2.2.2]:



Ionization is used in a sputter process. Here positive ions are accelerated from the plasma and towards the sample to be etched. If sputtering is the only method used for etching, then each ion hitting the sample surface will transfer energy to many target atoms, but usually only release one of these from the surface. This can be seen if we look at the sputtering yield, γ (atoms sputtered pr incident ion) [5.2.2.3] [5.2.1.2]:

$$\gamma_{\text{sput}} \approx \frac{1.9}{U_0} \cdot \sqrt{f} \cdot \left(\sqrt{\frac{E}{1000}} - 0.9 \cdot \sqrt{U_0} \right) \quad (6)$$

Here the approximation relation, f , for large ions is:

$$f \approx \frac{2 \cdot Z_t}{\left(\frac{Z_i}{Z_t}\right)^{2/3} + \left(\frac{Z_t}{Z_i}\right)^{2/3}} \quad (7)$$

Where:

U_0 is the surface binding energy [5.2.2.2] [eV]

E is the incident energy [eV] (A typical value is found in [5.2.2.3])

Z_i is the atomic number of the incident atom

Z_t is the atomic number of the target atom



By inserting values for silicon etching with fluorine we have:

$$\gamma_{sput} \approx \frac{1.9}{2.353eV} \cdot \sqrt{\frac{2 \cdot 14}{\left(\frac{9}{14}\right)^{2/3} + \left(\frac{14}{9}\right)^{2/3}}} \cdot \left(\sqrt{\left(\frac{600}{1000}\right) keV} - 0.09 \cdot \sqrt{2.353eV} \right) \approx 1.88 \frac{\text{atoms sputtered}}{\text{incident ion}}$$

By itself this method is slow and it is therefore often used together with chemical etching – like in plasma. Here ions are a minor component, representing around 1 ion pr 100.000 molecules [5.2.2.2] only, and therefore not being used so much to etch the silicon directly, as to release etch products (fx. SiF₄) from the surface. The sputtering is very directional though, and can be used for anisotropic etching. Furthermore sputtering is very unselective which can also be seen in the formula (6) where $f \approx Z_t$, and so because we take the root of f , only small changes will occur with change of mass.

The main etching of a sample (silicon wafer) is done by chemical etching. Here we need fluorine atoms as explained above. These we can get from dissociation in the plasma. This etch is isotropic and the etch rate can be found using the following equation [5.2.2.3]:

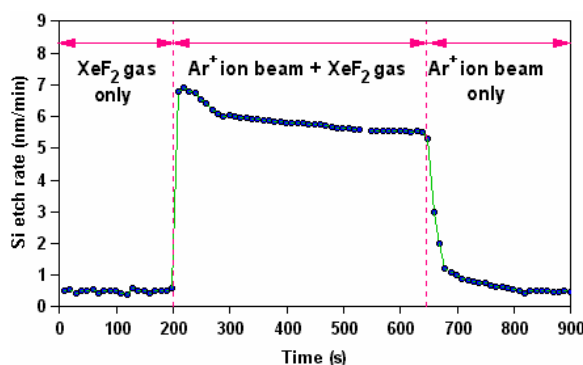
$$E_{Si}[\text{Å} / \text{min}] = 2.86 \cdot 10^{-12} \cdot n_{FS} \cdot T^{1/2} e^{-1248 / T} \quad (8)$$

Where T is temperature [K] and n_{FS} is fluorine density near the surface. At room temperature (300K) and a typical F-density of $\left(3 \cdot 10^{14} \frac{1}{cm^3}\right)$ we get an etch rate of:

$$E_{Si} = 2.86 \cdot 10^{-12} \cdot (3 \cdot 10^{14}) \cdot 300^{1/2} e^{-1248 / 300} = 232 \text{ Å} / \text{min}$$

However, when F-atoms bind with Silicon it creates a thin film (2-5 monolayers) of SiF_x on the surface, which prevents further etching. Now diffusion of F-atoms into the surface creates the etching, which makes it a far slower process – hence the combination with sputtering in plasma. Excitation of free radicals, molecules or atoms helps speeding up the etching process.

By creating plasma we exploit the benefits of both sputtering and chemical etching in a combination far more reactive than each process alone [5.2.2.3]:



[5.2.1.4] Figure 2.1.1: Ion enhanced plasma etching.

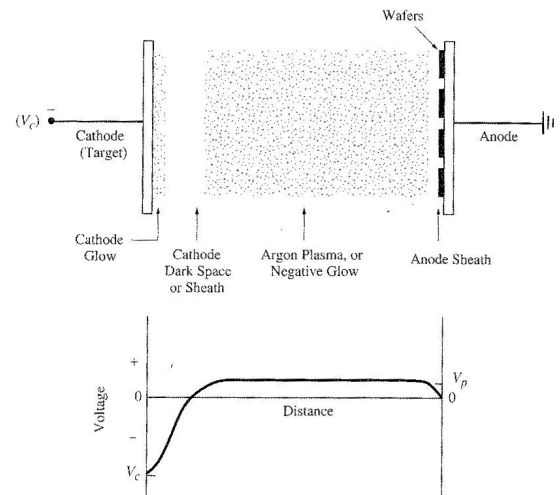
This graph show the etch rate for chemical, physical and combined etching. On the left side of the graph, only chemical etching occurs. On the right side only physical sputtering takes place. In the middle both chemical and physical etching combines in an etching process by far faster than the sum of the two etches by themselves.



Now with a high incident flux of fluorine atoms, a single 1kV argon ion can remove 25 silicon atoms from a silicon surface [5.2.2.3] instead of ≈ 1 . Even though this is demonstrated for argon, the same effect applies for plasma etching with fluorine.

2.1.1 DC Sputter Deposition

To better understand the ICP RIE (see below), it is easier to explain how the DC sputter works and then advance from there. In the DC sputter we have two equal sized electrodes (conductive). The wafers are placed on top of one electrode (anode) which is grounded, and then a negative voltage is applied to the other electrode (cathode). A gas (for instance Argon) is then pumped in between the electrodes. In this system the point is to sputter off material from the cathode (target), and then deposit it on the wafers. When the power is turned on and gas is applied it creates plasma (positive ions and electrons), by exciting and ionizing the argon atoms. It is the photon emission from the excited argon atoms that makes the plasma glow.



[5.2.2.4] Figure 2.1.2:
On top is the plasma distribution.
Below is the Voltage distribution

Now, the positive ions are attracted to the negatively applied voltage and thus travel left (if we look at figure 1.2.2) towards the cathode. In the cathode dark space there is now many positive ions and only a few electrons. Therefore only few collisions between them happen, making this area appear dark because of the lack of excited atoms. When the positive ions reach the target, they can sputter off material (for instance aluminium atoms), which then travel right to the wafers and deposit [5.2.2.4].

If we look at the voltage distribution between the electrodes (figure 1.2.2), we have on the left the negatively applied voltage rising as we go right. In the dark space the positive ions act as current carriers and so we have the highest voltage rise here. This rapid change also accelerates secondary electrons from the cathode to the plasma, and thereby sustaining it.

In the negative glow area both ions and electrons will randomly hit the plasma surface and escape the plasma. Since, however, the electrons are much faster than the ions, they will escape more often, leading to the plasma being positive in respect to both the electrodes.

So by having this asymmetric voltage distribution, we can accelerate positive ions towards the target and sputter it, as long as the electrodes are made of a conducting material.

2.1.2 RF Sputter Deposition

When using DC voltage on insulating electrodes, positive charges will build up by the electrodes, causing the voltage drop to be too small to sustain the plasma. In RF sputter deposition we couple the RF voltages capacitively. This means that we do not need conductive electrodes, since the positive charge build up, is countered by electron bombardment over each cycle. This bombardment happens because the electrons again are faster than the positive ions, and thus can keep up with the very high change (usually 13.56 MHz), whereas the ions can not. Hence more electrons than ions travel to the electrodes, creating a voltage distribution as can be seen by the solid line in figure 1.2.3. Even though the heavy positive ions do not travel towards the electrodes in response to the high RF frequency, they are attracted due to the DC potential difference that can be seen at the electrodes.

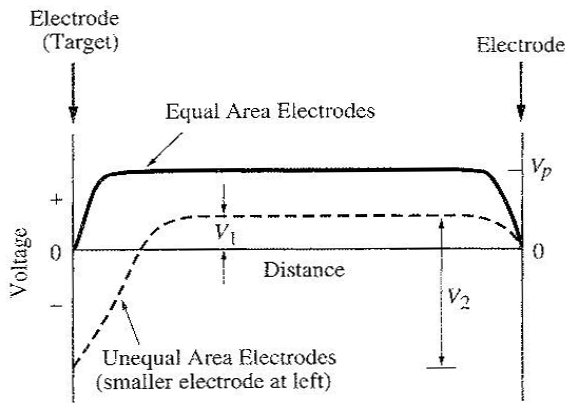


Figure 2.1.3:
Voltage distribution in RF powered systems

A change of electrode size, however, can change this distribution to resemble the one from DC sputtering, because a smaller area will give a larger voltage drop. So by making the cathode smaller and at the same time also connecting the anode to the chamber walls (grounded), to give it a larger effective area we now have a system resembling the DC sputter which also works for insulating materials.

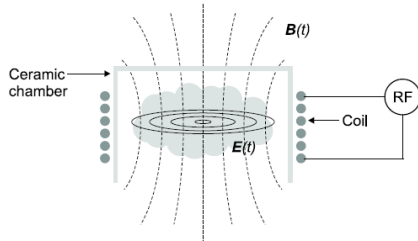
2.1.3 Reactive Ion Etch (RIE)

The difference between the RF sputtering and the RIE, is quite simple. In RF sputtering, we attract the positive ions towards the left electrode (the one without wafers) to sputter off atoms that can be condensed on the wafers on the right. In RIE we make the electrode holding the wafers the small one, and ground the other one. Now the positive ions are attracted towards the wafers and sputter them directly. This is used when covering the wafer with an etch mask, in order to only etch the desired places. The RIE method not only uses the sputtering for etching, but also the chemical neutral reactive species (free radicals). As described in the first sections of this topic, this combination is by far the fastest etch method, while still being directional.



2.1.4 Inductively Coupled Plasma Reactive Ion Etch (ICP RIE)

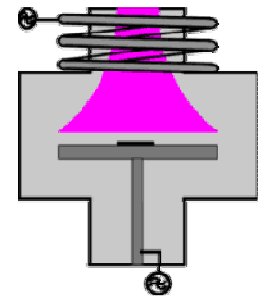
To advance even further than the RIE the ICP RIE was invented. By adding a separate coil operating at the same frequency (13.54 MHz), induction instead of capacitance can be used to create the plasma (figure 1.2.4):



[5.2.2.5] Figure 2.1.4:
ICP RIE separate coil

By surrounding the chamber with a coil it will act as a transformer, with the plasma inside as the secondary coil. This will accelerate the electrons and ions and make them collide more often, creating a higher density. The platen, upon which the wafers lie, is still powered, though independently, from the inductive system, and therefore still creates a directional attraction towards the wafers.

In a RIE process you can increase the power to get a higher density, but at the cost of higher ion energy, which causes more substrate damage. In the ICP RIE these two processes are separated, and a higher density can be achieved in the inductive area, without changing the sheath bias (affects ion energy) at low pressures. In RIE processes heightening the pressure does the same, but it also leads to a more isotropic etch, due to more collisions in the sheath, deflecting the etchants more often. Hence the ICP RIE is more selective, has a higher density, giving a faster etch, while maintaining directionality.



[5.1.1.4] Figure 2.1.5:
ICP RIE chamber overview

In this figure 1.2.5 it is easy to get an overview of the different properties that affect the different processes. By adjusting the two most important parameters: pressure and energy, we can get a more anisotropic or selective etch process. The higher we get the more of the etching is caused by sputtering. Likewise the lower we get the more chemical an etch do we get:

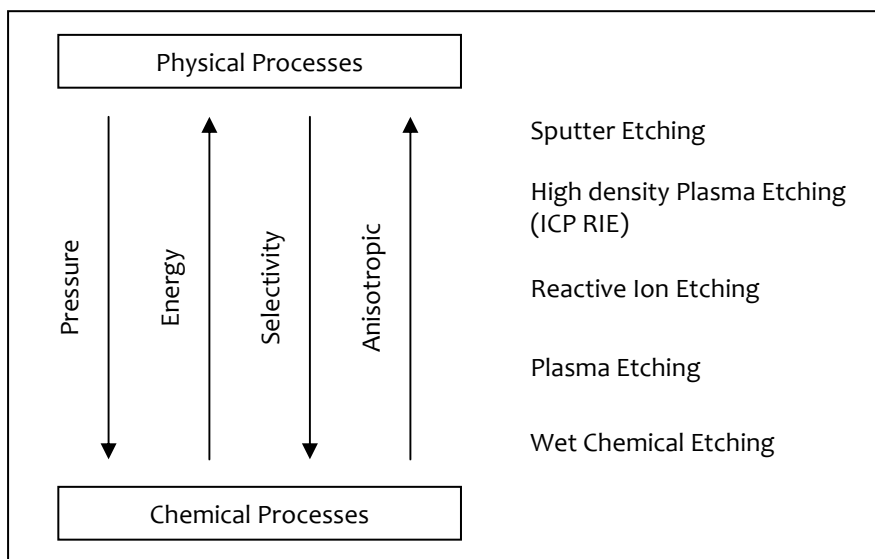


Figure 1.2.6: An overview of the different processes and properties



2.1.5 Bosch Process

When etching with the ICP RIE, a technique called the Bosch Process is used (sometimes also referred to as time-multiplexed deep etching (TMDE)). Basically etching gas (SF_6) and a passivation gas (C_4F_8) is let in to the etching chamber in a shifting process. By doing this we get a very anisotropic (vertical) etch. First everything is covered in a protecting layer from the passivation gas. Then a nearly isotropic etch is made in all areas using the etching gas. However, this etch does not etch through the passivation layer, except at the trench bottoms, where the directional sputtering helps to penetrate the protective layer. The passivation gas is then used again, then the etching gas, and so this gas shift continues during the whole etch process. See figure 1.2.7.

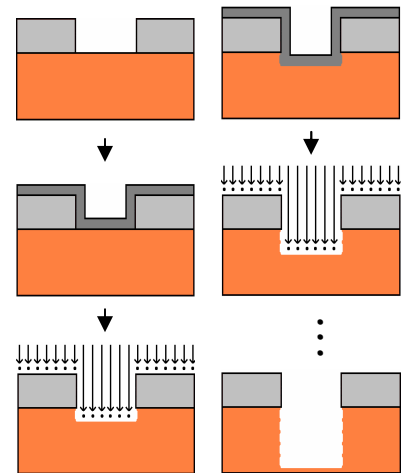


Figure 2.1.7:
Bosch process step by step

2.1.6 Error minimization

Every time a new etch process is being run, there is a difference compared to the wafer etched last time. This error can be caused by different effects like: conditioning, uniformity (pattern density), reproducibility and oxygen.

Conditioning is used to remove contaminants attached to the chamber walls, and also heat up the etching chamber since temperature has an effect on the process [5.2.1.5]. The ICP RIE I work with, has a heated main chamber (always 150°C). Therefore it should not be necessary to do any conditioning in my process, since contaminants will not attach to the hot chamber walls, and the temperature is monitored and fixed so that there should be no changes due to long time use.

If the pattern to be etched, is etching away more material in the middle than at the edge, then it will have a faster etch rate at the edge [5.2.2.5]. This is due to the extra fluorine atoms not being used where there is no edge pattern. Since my mask design does not have any large etching areas, and is pretty symmetric, I do not see the need to fill empty space in between the platforms in order to get a more uniform etch.

In the course of my project I will need to create new wafers for study from time to time. Therefore a large batch (5-10 wafers) will be made each time new platforms are needed, in order to minimize reproducibility errors. These batches may be etched using different time intervals, but should be etched one by one shortly after each other.

Adding an oxygen flow to the etch flow, may improve the etch speed, since the oxygen atoms bond with the sulfur atoms, preventing recombination with flour, hence creating a larger flour density. This could help make the scallops smaller, or allowing for adjustments in parameters that causes design error, like trenches created by too low pressure or too high ion energies. The SF_6/O_2 ratio should be around 7:3 in order to get the fastest etch [5.2.1.6]. However, adding oxygen will speed up etching of the protective photo resist mask, and therefore result in a poorer selectivity.



2.2 Test platform

The test platform can be divided into three groups: platform base, sealing, and connectors. The silicon base is the main platform in which the channels used for hydrodynamic focusing are etched. Since these are open channels, a lid is needed, which is added in the sealing process. Finally connectors for hoses used to pump in specimens, has to be placed on top of the seal.

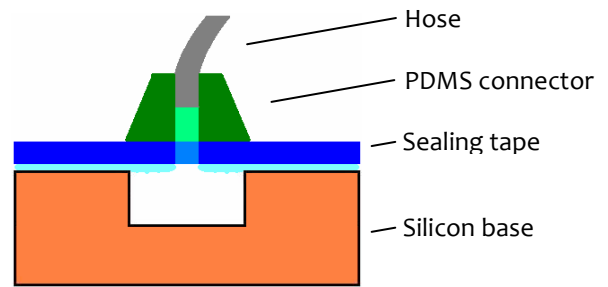


Figure 2.2.1:
Overview of the assembled test platform

2.2.1 Platform base

The platform base structure is a silicon wafer in which channels of appropriate sizes have been etched. After etching it has been cut out in pieces representing a platform base for a single hydrodynamic focusing system. This method requires the silicon base to be part of the system. If instead an inverse lithography step had been used before etching, we would have had silicon hills in place of valleys. By coating these hills with liquid polydimethylsiloxane (PDMS), and then hardening it, a PDMS base could have been made.

To get the best possible flow through the channels, low resistance is important. This can be achieved by changing channel sizes and lengths. Another method could simply be to coat the entire surface with a silicon dioxide layer, by oxidizing the silicon in oxygen plasma. This will make the surface hydrophilic, whereas silicon is hydrophobic. To distinguishing between hydrophilic and hydrophobic materials, we can look at a liquid drop in contact with the surface. If the angle of the liquid is below 90° it is considered hydrophilic. Above 90° it is considered hydrophobic [5.1.2.6]. See figure 2.2.2 below:



Figure 2.2.2: Left is a water droplet on a hydrophilic material; right a water droplet on a hydrophobic material

This effect happens because water molecules are slightly polarized [5.1.2.7]. Hydrophilic surfaces are also polar and can bond with the hydrogen atoms of the water molecule. This will make the water spread out on the surface, giving it a low contact angle. If the surface is non-polar then the water prefers to bond with “itself” and thereby repels the surface [5.1.2.8], without wetting it. So to get the water flowing easily in the channels, and not resist entering, the hydrophilic surface is preferred which will give the lowest resistance.

2.2.2 Sealing

Sealing the microchannels and platforms can be done in different ways. The channels created, since etched in silicon, are open on top, and therefore no liquid can be pumped through. One way to seal the channels/platforms is to glue tape on top of the channels. Another method is to create a lid of PDMS. Both methods have advantages and disadvantages.

If tape is used for sealing, a very smooth surface can be achieved. Also this lid is very thin, and is thus excellent for microscopy use. It is easy to attach, but one has to take care not to scratch it in the process. But even though the tape itself is fast to attach, it will require external connectors, which compared to the PDMS solution, can be harder to match exactly over the inlets and outlets. Also such extra connectors give rise to possible liquid breach errors, between the tape and connectors. Another thing is that consequent use of liquids in the systems for hours at a time, can cause the tape to release itself from the silicon surface. Lastly the tape might be autofluorescent. If this only occur for certain wavelengths, then using a dye which reflects waves at a different wavelength in combination with wavelength filtering, should still give good images.

When using PDMS as a lid, it has to be made separately and attached after hardening. PDMS has a low viscosity [5.1.2.9] and so it would clog up the channels if it is applied directly onto a wafer with channels in it. However, when using PDMS for a lid, connectors are not needed, since the PDMS can be pierced by a needle at the locations needed, making a perfect fit for hose connection. The only problem with this method is that the PDMS has to be thick enough for the hose not to be pushed out. Making the PDMS layer thicker, makes it harder to look through it in a microscope though, and so may lead to a poorer measuring resolution. Also bubbles appear in the hardened PDMS which can block the line of sight, from microscope to sample. Using a thin layer of PDMS and combining it through slight oxygen plasma etch [5.2.1.7] of the surface, with connectors also made of PDMS, a better result may be possible. This would also reduce the chance of bubbles getting in the way of viewing. Lastly using the oxygen plasma method can also be used to bond the PDMS with the silicon, to make a stronger connection, resulting in fewer leaks.

If autofluorescence is no problem when using tape, then this is the method that will be used for my channels/platforms. The use of 50-100x objectives in the microscope, (for the ones we have available) requires the lens to be very close to the sample. Using tape for sealing, also gives a more certain smooth surface. The tape going to be used is ARcare® 7815 (appendix 6.1.5), which is a clear adhesive film. It is made of three layers: A substrate layer consisting of 50.8 µm clear polyester film, a 25.4 µm adhesive layer which is hydrophilic, and a liner consisting of siliconized polyester release film. The liner is removed before use, and when applied the tape has a 95.9 % light transmission.



(Appendix 6.2.2) Figure 2.2.3: ARcare® tape composition

2.2.3 Connectors

To be able to pump sample and sheath liquids into the platforms, connectors between hoses from the syringe pump, and the channel inlet/outlets are needed. These connectors are made from PDMS, in a fabrication procedure similar to a method found on the internet [5.1.1.5]. A double-sided adhesive tape is used to bond the PDMS to the sealing tape. However this connection is not very strong and so a filter paper with large enough pores for the PDMS to penetrate, is placed in between. These pores shall according to the internet article be between 2-8 μm in width. However I have filter paper with 20 μm large pores available at school (Whatman 41 [5.1.1.6]), which is also large enough for the PDMS to penetrate, so this will be used.



Figure 2.2.4: PDMS ready for cutting off connectors

The PDMS itself is Sylgard® 184 silicone. This is a silicone base and catalyst mixed in a 10:1 ratio [5.1.1.7]. When mixed together in a container, the silicone starts to harden. The rate with which it hardens depends upon temperature, and so it is heated at 50°C on a hot plate for 4 hours, and then left overnight to be sure it is fully set.

To pump water through the connector a hole must be made. This can either be done using a needle or a drill. Using a needle gives the best grip between the hose and connector, but it can be hard to get the hose into this socket. Using a drill on the other hand can leave behind crumbs, but since it is easier to operate with, this method will be used for my connections. Now all that is left is cutting out the PDMS into small connector pieces, which with success may be shaped as small pyramids. This will make the contact area between connector and sealing tape the same size, but with the benefit of being able to move the microscope closer to the channel crossing.



Figure 2.2.5: Connector ready for platform placement

2.2.4 Syringe pumps

The syringe pumps used in this project are PHD 2000 [5.1.1.8], from Harvard apparatus. This model is capable of using two syringes simultaneously. With two of these pumps one of them can be used for the sample flow using one syringe, and the other pump can be used for the sheath flows, which shall have the same flow rate in both channels. The syringes used will be in sizes adapted to how much liquid is needed for the specific channel. The pumps have a high working range, and so most of the syringe sizes can be scaled to pump in liquid in the desired working scale.

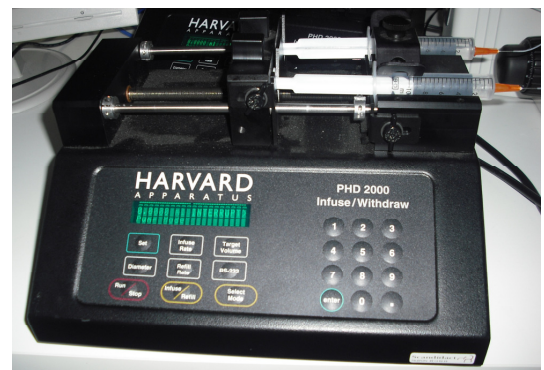


Figure 2.2.6: One of the syringe pumps mounted with two 10 ml syringes.



2.2.5 Dye color

To be able to distinguish the sample flow from the sheath flows, a dye is needed. However, the dye needed depends upon what is used for detection. If a normal lamp is used for observation we need a dye with a powerful color that helps us distinguish the sample flow from the sheath flows. For this Eosin [5.1.2.10] will be used. If that does not work and a UV light source is being used, then Trypan blue [5.1.2.11] will be used, since it is fluorescent to this light. Eosin is pink-orange and normally used to dye cytoplasm in cells. Trypan blue is as the name says blue, and can also be used for viewing in normal light. It is normally used to dye cells, but can only dye dead cells and not live ones. If neither dye can be seen in the microscopes, then fluorescent beads can also be an option.

The dyes can either be used in the sample channel, or in the sheath flow channels. For the main use the dye will be pumped into the sample channel, in order not to exhaust the supply available. The liquid used for the sheath flows, is going to be demineralized water. Since the dyes used in the sample channel, will be thinned plenty in water, we can assume the whole system, including the sample channel, is going to have the same viscosity as water.



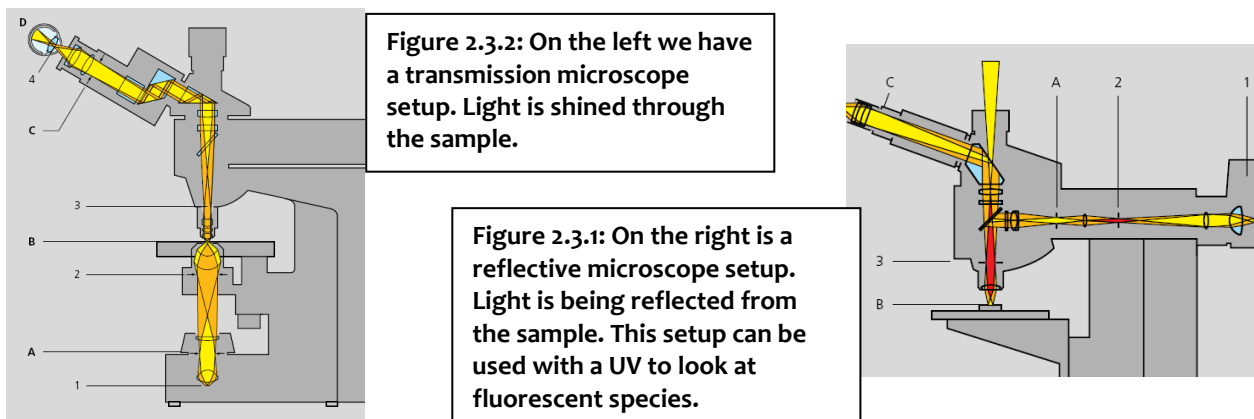
Figure 2.2.7: Trypan blue/water mixture recollected after use

2.3 Microscopy

To examine the channels fabricated in the cleanroom and also to study the hydrodynamic focusing, different microscopes are used, depending on the information needed. The largest channels I shall create are 200 μm wide, and can therefore easily be spotted by the naked eye. But the small channels and also details like edges, structure and flow focusing are so small that I need different tools to study them:

2.3.1 Optical microscope

The optical microscope is by far the fastest microscope to use. It is easy to operate and has lenses ranging from five times magnification to a hundred. It can be used with the light coming from the bottom up or by the use of reflected light.



Normally using light from the transmission microscope can be an advantage. This is because unlike the reflective microscope where the condenser lens is integrated into the microscope and also the aperture diaphragm only needs to be adjusted once, these lenses can be adjusted manually to catch the most light, which gives the best picture. Also the transmission microscope can be used with darkfield microscopy, where the inverse picture is made, giving a better contrast. However, since the channels I create are etched in opaque silicon, they can only be viewed using reflected light. This light is either going to be ordinary bright light created from a 50W halogen lamp or UV light reflecting excited fluorescent light, depending on what gives the best results, in my setup.

This approach will be used to help map the hydrodynamic focusing. The fact that the images can be viewed realtime is important when liquids are being pumped into the channels and fast changes have to be recorded.

The magnification of an optical microscope depends normally on the objective, and eyepiece using the following formula [5.2.2.6]:

$$\text{Total magnification} = \text{objective magnification} \times \text{eyepiece magnification}$$

But when using a camera for taking pictures it depends on the camera magnification instead of the eyepiece.



2.3.2 Navitar setup

PhD student, Casper Kunstmann-Olsen, is currently working on a laser-setup for detecting and counting beads in a microchannel. Here is a picture of his setup so far:

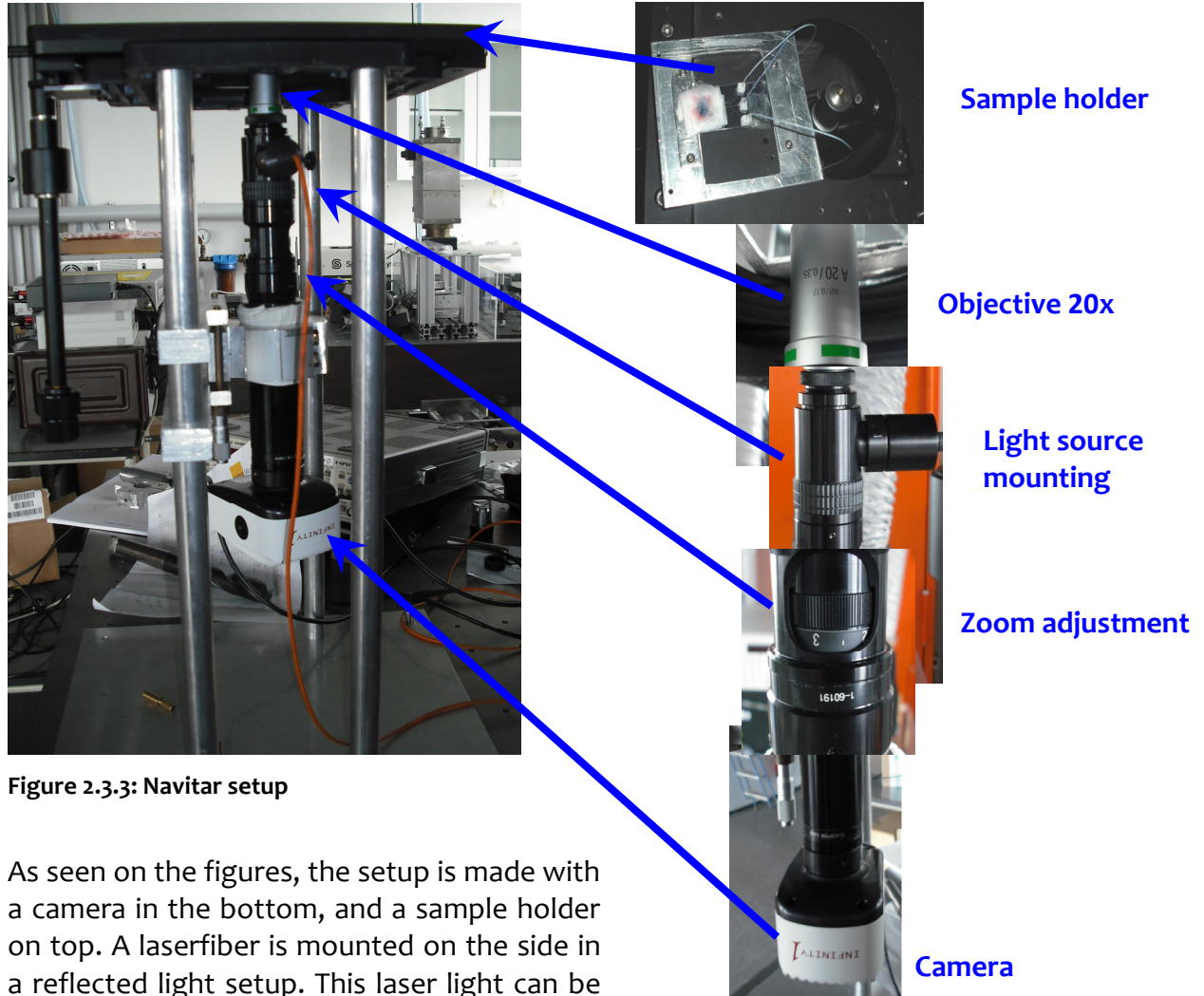


Figure 2.3.3: Navitar setup

As seen on the figures, the setup is made with a camera in the bottom, and a sample holder on top. A laserfiber is mounted on the side in a reflected light setup. This laser light can be used to take fluorescent pictures, but unfortunately something in the path of the laser light causes it to radiate a spotted light beam, and hence it will not be used:

Figure 2.3.4: Each piece of the Navitar setup brought out in a collage.

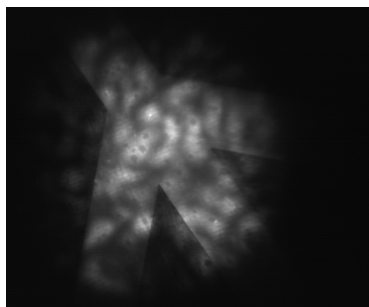


Figure 2.3.5:
Distorted laser image of channel crossing

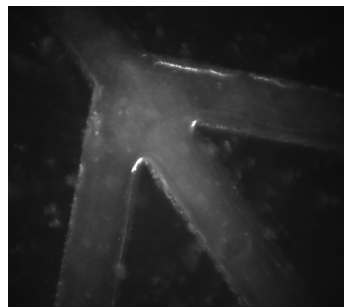


Figure 2.3.6:
12V 50W Halogen lamp

By removing the laserfiber and instead mount a bright light lamp, brightfield microscopy can be made with the light almost centered in the specimen plane. An adjustable lens in the middle can change the magnification of the setup. The objective at the top magnifies 20x.

2.3.3 Fluorescence microscope

The fluorescence microscope works pretty much like the optical reflected light microscope. Instead of a normal lamp though, a mercury lamp is used. Also the beam splitter normally used to direct reflected light to both camera and sample, now acts as a filter. It reflects almost all short waveled light down to the sample. When longer waves arrive from the sample, they are let though. See figure 2.3.6: below:

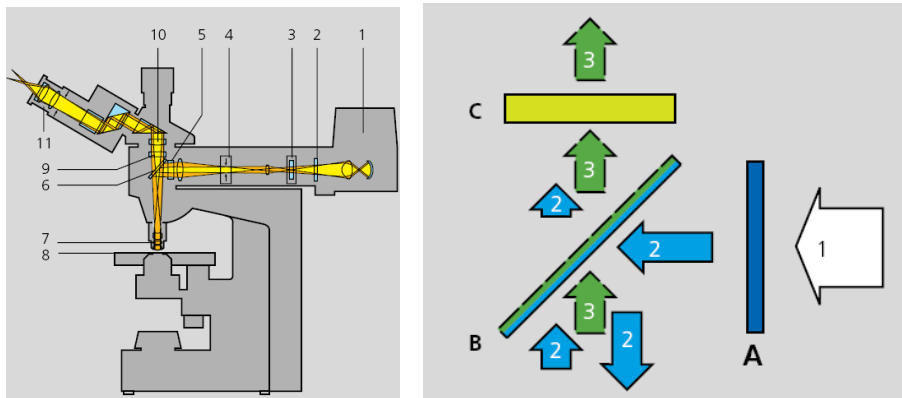


Figure 2.3.7: On the left is a fluorescence microscope. On the right is the beam splitter.

Now when fluorescent specimens are exposed to light of a certain wavelength, they absorb the light and then after an extremely short period (sometimes billions of a second), they send back the light with 20-50nm longer wavelengths [5.2.2.6]. This usually gives a shift (Stokes shift) in the color reflected, going from left to right in the figure 2.3.8 below:

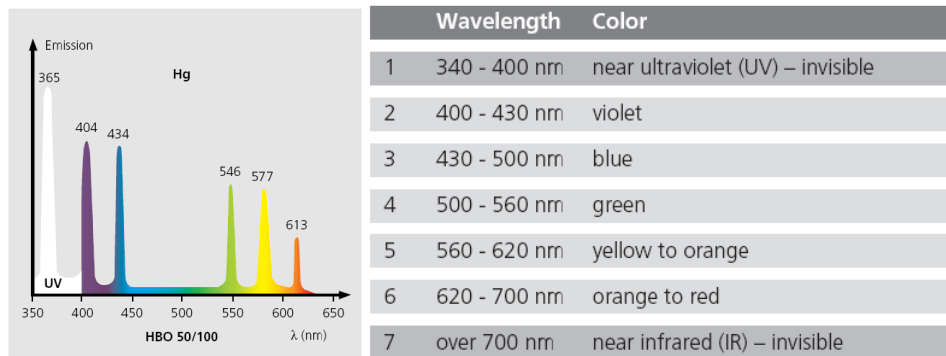


Figure 2.3.8: Wavelengths for the different colors.

The fluorescence microscope we have available comes with three different filters making multi-fluorescence available. By using these filters, specimens with different fluorescent properties can be viewed. Also the microscope has different objectives mounted, making it possible to change the magnification between: 5x, 10x, 20x, 50x and 100x. If the light intensity is to low, using immersion oil will help send the light into the microscope. Also doubling the objective aperture angle, will give approximately four times as much light.



2.3.4 Profilometer

The profilometer is used for precise measuring the depth along a line. It is fairly fast, and works by dragging a tip across the wafer, and then when hitting a bump or a trench, the tip will lift or lower a lever, that converts the movement into electrical signals. This kind of measure gives a cross section view along a single line. The software belonging to the apparatus can then be used to calculate the exact depth of the channel. This is very useful for shallow or wide channels, but as I need to measure narrow channels with a depth of up to 200 μm , it might be a problem. The profilometer's tip and tip mounting are too big to enter the small channels and reach the bottom, and so false measurements can be made.



Figure 2.3.9: A picture of resist thickness taken with the profilometer.

I will therefore mainly use the pictures gathered in the profilometer for measuring thickness of resist, which is very shallow (1-2 μm deep), or comparing the depths of some of the shallow channels (25 μm).



Figure 2.3.10: Stefan Johansen operating the SEM

Scanning Electron Microscope (SEM)

The Scanning Electron Microscope is using an electron beam to create a picture of a surface area. This is done by scanning an electron beam across the surface in a raster scan. Depending on the conductivity of the material looked at, it can give pictures magnified to a great level (250k). As I am looking at silicon, which is a semiconductor, I should have no problem creating good images. If the images appear to poorly though, coating the wafers with a very small layer of well conducting gold should help optimize the image.

To be able to measure the channel depths etched, test wafers will be broken, so that the cross sections of the channels can be studied. This will also give a picture of the structure layout.

By breaking the wafer for use in the SEM, it will be rendered useless for hydrodynamic focusing, since the break up has to be done in the middle of a channel. Therefore test channels should be implemented on the wafer mask, making it possible to break out some of these channels without destroying the platform used for the cytometry.

The SEM can be used in various modes. When using it in TV mode the resolution is not so good, but the gain is a real time picture. When something is found worth saving, you just change the resolution to high, and wait for the result. This makes it a good and fast method for examining the etched wafer channels. However it operates the electron beam in a vacuum chamber and is therefore not suitable for studying the hydrodynamic focusing.



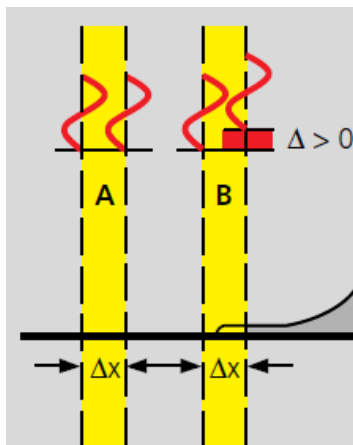


Figure 2.3.11: Polarised light shifting phase, because of different reflection heights.

2.3.5 Interference microscope

The interference microscope works by either sending out waves at the same phase. For simplicity we look at two waves sent (case A) in figure 2.3.12. If one of the waves is reflected from a different height than the other (case B), then this wave will be phase shifted. On the way back to the microscope, these waves can interfere with each other, changing path differences into variations in intensity that can be measured.

When doing measurements with the interference microscope, you can choose to operate it with white light (containing a lot of different frequencies) or with red light only (contains only one frequency). The white light has, because of its many frequencies, the advantage that it can differ from top till bottom of a large step for instance a channel. Because red light can only detect changes within one frequency, you get a more intense light and can detect smaller changes. However, with this method a phase shift of more than 360° will be measured as being back to zero height and so it continues from there:

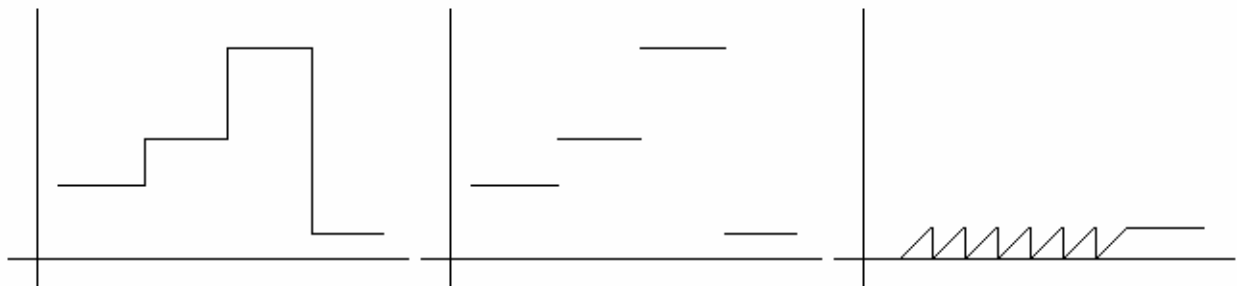


Figure 2.3.12: a) a signal with varying step height; b) white light interference measurement; c) red light phase shift measurement

3 Realization of the microfluidic system

3.1 Mask design

In order to etch microchannels in silicon, a mask with the desired pattern must be designed and fabricated. This mask is then used in the lithography steps to imprint the pattern onto a wafer, either directly or with a negatively inverted image. By using the direct method channels will be etched directly. If the negative process is used, then everything but the channels will be etched. This can be useful if we are going to use the wafer for a stencil or a mold in fx. PDMS. Then the PDMS structure will be filled with channels. The mask itself is ordered from an external company (Delta Mask), and thus needs to take as much into account as possible. If the mask is insufficient, designing and ordering a new mask will cause time delays and may slow the whole project for a couple of weeks. The things that need to be considered are the following:

3.1.1 Wafer

The wafers used for fabrication are standard silicon wafers with a diameter of 10 cm (4"). To avoid scratches and defects caused by grippers and pliers, there should be an approximately 1 cm wide empty rim along the edge. This gives a usable area of 8 cm in diameter. The lithography machine has two microscope objectives placed 7.5 cm apart, so potential alignment marks should be placed here.

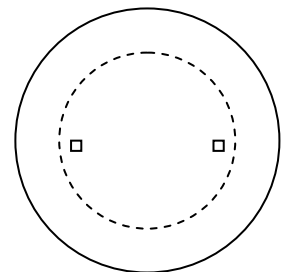


Figure 3.1.1: Wafer with scratch rim and alignment marks

3.1.2 Platform design and placement

The main microfluidic platform used for hydrodynamic focusing, is designed to resemble the commercial system, only without the channels used for sorting, as can be seen on figure 3.1.2 a. However since it is desired to investigate four different channel sizes, 25, 50, 100 and 200 μm , some of the platforms will have an angled exit channel (figure 3.1.2 b) to save space. By doing this a platform of each channel size can be fitted into every "corner" of the wafer, as shown on in figure 3.1.2 c. This even still leaves room for two of the straight platforms in the middle of the wafer. These shall both be 100 μm wide since that is the main width to focus on, and should therefore resemble the commercial system the most (figure 3.1.2 d). Lastly there shall be some straight channels, having a width similar to each platform. These can then be used for tests without ruining the platforms (figure 3.1.2 e):

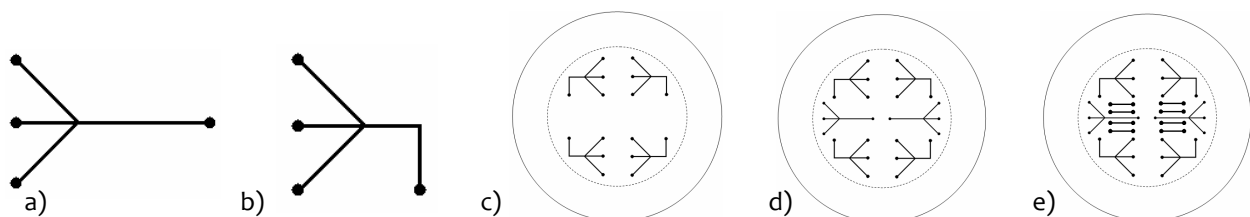


Figure 3.1.2: a) design resemble the commercial system; b) space conserving equivalent to the commercial system; c) placement of each channel size using the space saving system; d) Two straight 100 μm channels added; e) Measure channels placed for extra measuring possibilities.

3.1.3 Channel structure

When a mask has been made the width of the channels will be determined by that mask, and therefore cannot be changed later. As mentioned above my channels should be either: 25 μm , 50 μm , 100 μm or 200 μm wide. To easy be able to compare results between the different channel sizes, the depth shall be the same as the width. Hence a cross-section of the channels gives a square figure:

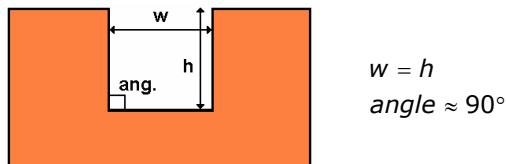


Figure 3.1.3:
 Channel cross-section

The longer the channel, the longer the fluid has to be pumped, hence the higher a pressure is needed. We can make a fluidic analogy to Ohm's law [5.2.1.8]:

$$\Delta P = QR$$

Where: ΔP is the pressure drop [Pa]

Q is the volumetric flowrate [$\mu\text{L}/\text{min}$]

and: R is the flow resistance, depending on the fluid velocity profile [$\text{Pa} \cdot \text{s}/\text{m}^3$]

For a square channel profile the resistance can be calculated using the following relation:

$$R = \frac{12 \cdot \eta \cdot l}{h^3 \cdot w} \quad \text{where:}$$

η is the fluid viscosity [$\text{Pa} \cdot \text{s}$]
 l is the length of the channel

This means that whenever the channel gets longer, the resistance increases requiring a larger pressure to pump the fluid all the way through. If the pressure gets too high we risk that the sealing or connectors will be pushed off the platform and rendering the channel useless. For starters I will make my channels 20 mm long giving a pressure drop of:

$$R = \frac{12 \cdot 0.00089 \frac{\text{Pa} \cdot \text{s}}{\text{m}^2} \cdot 20 \text{mm} \cdot 10^{-3}}{(100 \mu\text{m} \cdot 10^{-6})^3 \cdot (100 \mu\text{m} \cdot 10^{-6})} = 2.136 \cdot 10^{12} \frac{\text{Pa} \cdot \text{s}}{\text{m}^3}$$

$$\Delta P = \left(\frac{250 \frac{\mu\text{m}}{\text{min}} \cdot 10^{-9}}{60} \right) \frac{\text{m}^3}{\text{s}} \cdot 2.136 \cdot 10^{12} \frac{\text{Pa} \cdot \text{s}}{\text{m}^3} = 8900 \text{Pa} = 0.089 \text{bar}$$

By measuring the flow making the connectors leak, this number will help me adjust channel lengths in future designs.



3.1.4 Alignment and cutting marks

In the case the mask design is later going to be used in a multilayer process, two alignment marks is places on each side (east-west) of the mask. Right now it gives no benefit, but since it is quickly drawn it was chosen to include.

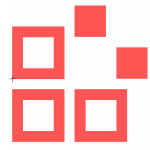
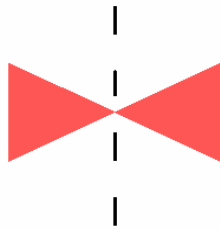


Figure 3.1.4:
Alignment marks



Lastly cutting marks are added around the wafer. Every platform is deliberately placed so that they all can be cut out and used from the same wafer. The non-square channels will not be used for gathering results, but they can still be helpful for testing. Hence the cutting marks are placed along the empty rim boundary, to make it easier to break the wafer once it is ready for testing. The cutting marks are only placed in the x and y directions, which is needed for the breaking to follow the crystal structure of the silicon wafers.

3.1.5 The real mask

The final mask design can be seen in appendix 1. After receiving the mask, I examined it for errors in the optical microscope. No errors of importance were found. What appeared on the west most 100 μm straight channel to be a scratch, was only a little dirt, and could gently be scraped of.

3.1.6 Platform fabrication process: Creating channels in a silicon wafer

After receiving the mask, silicon platforms need to be made. The processes involved in this fabrication are all done in the cleanroom. This is to avoid contaminants roughening or ruining the channels. Also, some of the processes require a certain humidity and/or temperature and lastly most of the required equipment is placed here. Different steps need to be executed in the fabrication process of these silicon platforms. These steps will be described below, in the order with which they are performed.

3.1.7 Preparing wafers for the ICP RIE

Before the wafers can be etched in the ICP RIE, the mask design needs to be imprinted on top of it. The steps used to do this, are the same for all wafers created and is done by: hexamethyldisilazane (HMDS) [5.1.2.12] coating, photo resist coating, baking, lithography exposure and development.

The HMDS coating is applied in an oven. The wafers are heated at a temperature of 120°C, in order to remove moisture from the surface. Then HMDS is let into the oven, long enough to cover the surface. The HMDS is used to get the photo resist, applied in the next step, to bond better with the wafer.



Figure 3.1.6: HMDS oven ready for work



Figure 3.1.7:
Spin coater

After cool down of the wafers, they are placed in the spin coater one at a time. Here the photo resist AZ 5214E [5.1.1.9] is added to the wafers. When the resist is being applied onto the wafer, it should not be spinning. Then afterwards the wafers are spun slowly (500 RPM for 5 sec) to distribute resist to the entire wafer, before finally spun at 4000 RPM for 30 seconds, in order to achieve a layer thickness of about 1.4 μm [5.1.1.9]. By spinning on the photo resist, we get a very uniform layer, typical with variations of only 5-10 nm [5.1.2.13].

Before exposing the wafer to UV light, during the lithography step, prebaking it on a hotplate is done to get rid of excess solvent. This has to be done at a temperature below 110°C, since temperatures above this limit will cause the photo resist to cross link (harden) [5.1.1.9], which is used in negative lithography processes. The prebaking is therefore completed at 90°C for 60 seconds.



Figure 3.1.8:
Wafer prebaking
on hot plate



Figure 3.1.9: Mask aligner

The lithography process is done in the mask aligner. It uses a Hg lamp with a wavelength of $\lambda = 365 \text{ nm}$. By shining UV light through the designed mask, the exposed areas (channels) will be soluble in the developer. If we wish to make the opposite process (negative), we should first expose the areas we want to keep, then reversal bake at 120°C , to cross link these areas, which will make them almost insoluble. Then giving the wafer a flood exposure makes the areas not cross linked, soluble in the developer. This method is better for lift-off processes. Due to previous experience all wafers will be exposed to UV light for 3 seconds each, using soft contact mode.

Before exposing the wafers in the mask aligner, the alignment marks will be fixed east and west. This is to make sure the wafer afterwards can be broken in the directions of the crystal structure, which gives a very clean cut.

The developer used for the next step is a fast, high resolution developer called AZ 351B [5.1.1.10]. It is mixed with deionised water in a mixture proportion of 1 part AZ 351B and 4 parts deionised water. With this combination, a wafer with approximately $1.5 \mu\text{m}$ resist needs to be covered for one minute at $22^\circ\text{C} \pm 1^\circ\text{C}$.



Figure 3.1.10: Me developing wafers

The wafers are now ready for etching in the ICP RIE. A sum up of the preparation process can be found in appendix 6.1.3. Before the etching the thickness of the resist is measured on a wafer, to make sure, it is the correct depth:

	Thickness	Deviation
Channel 25 μm east	1.590 μm	1.3 %
Channel 25 μm west	1.570 μm	0.0 %
Channel 50 μm east	1.575 μm	0.3 %
Channel 50 μm west	1.565 μm	0.3 %
Channel 100 μm east	1.565 μm	0.3 %
Channel 100 μm west	1.545 μm	1.6 %
Channel 200 μm east	1.575 μm	0.3 %
Channel 200 μm west	1.550 μm	1.2 %
Platform 100 μm east	1.640 μm	4.5 %
Platform 100 μm west	1.550 μm	1.2 %
Platform 25 μm (G1)	1.540 μm	1.9 %
Average	1.570 μm	1.2 %



Figure 3.1.11: Resist measurement on profilometer

As can be seen, the results are looking fine. None of the numbers stand out much, and they are all within a 5 % deviation of the average. Even though the average number is around 12 % higher than desired it is okay. What matters is that the thickness is not less than expected. When using the ICP RIE the photo resist is also etched (only very slow). Therefore it does not matter if there is too much resist on the wafer. If there is not enough, on the other hand, then the wafer will be etched in false places, after the resist breaches.



3.1.8 Recipe used for etching with the ICP RIE

The recipe that I will use for the ICP RIE will be based on a recipe received from Alcatel. This recipe use the Bosch process and has the purpose of creating square channels 22 μm deep. It is supposed to do this in 3 min and 30 seconds, so if a depth of 200 μm is required a run of approximately 32 minutes is necessary. For 100 μm deep channels it will be approximately half. The recipe will be the same used on all wafers, with the exception of the time they are etched, and looks like this:

	Etch step	Passivation step
Gas	SF_6	C_4F_8
Flow rate (active state)	300 sccm	150 sccm
Flow rate (inactive state)	0 sccm	0 sccm
Duration	3.5 sec	1 sec
Pressure	45 mbar	25 mbar
Source	1300 W	1300 W
Chuck power high	40 W	40 W
Chuck power low	0 W	0 W
Power high time	10 ms	10 ms
Power low time	90 ms	90 ms

Chuck position from source: 200 mm

Chuck temperature: 10°C



Figure 3.1.12: Mounting a wafer in the ICP RIE

In all a total of twelve wafers were created, in two batch processes: wafer 1-7 and then later wafer 8-12. The wafers were made like this:

Wafer no.	Etch time	Purpose
1	3 min 30 sec	Find etch rate
2	1 min 45 sec	Find etch rate
3	7 min 0 sec	Find etch rate

These wafers were created to estimate the actual etch rate. The etch time for wafer 1 is the initial recipes running time, supposed to give 22 μm deep channels. To get started I have chosen to halve and double this time period for wafer 2 and 3.

4	3 min 23 sec	25 μm channels/platform
5	defect	To large for ICP RIE wafer holder
6	6 min 46 sec	50 μm channels/platform
7	13 min 31 sec	100 μm channels/platform

These wafers were made to do initial testing. Unfortunately wafer 5 was too big for the wafer holder in the ICP RIE. I chose to neglect making the 200 μm deep channel, since I was not sure whether the resist was thick enough for such a deep etch, and also the purpose is to create hydrodynamic focusing in the scale of 1-10 μm which is much closer to the other measures and therefore easier to distinguish. In this batch I did not consider to give the wafers an oxygen plasma treatment in order to make them more hydrophilic. Both channels and platforms will be used for testing.



8	13 min 53 sec	100 μm platform
9	13 min 53 sec	100 μm platform
10	6 min 56 sec	50 μm platform
11	3 min 28 sec	25 μm platform
12	defect	No pattern in resist

These are the final wafers created for studying. This time an error happened with wafer 9. I seem to somehow have forgotten to expose the wafer before developing, because the wafer turned up blank afterwards. Again I skipped the 200 μm deep channels. Since I had poor experience using the 25 μm and 50 μm deep platforms, I want to focus on the 100 μm platforms and therefore create two of these. This time though, all wafers were etched shortly in the oxygen plasma barrel etcher after fabrication, and then sealed shortly after.

3.1.9 Etch rate for SF₆ on silicon wafers

To be able to calculate the etch rate, the etch depth must be measured after each etch. This is done using the interference microscope, since it is non-destructive and therefore can be used on the platforms directly without harming them. Also it is a fairly fast method. For starters the recipe used for the ICP RIE gives a good suggestion of how deep the etching is going to be:

$$\begin{array}{l}
 (0,0) \\
 y = a \cdot x + b \\
 \Downarrow 0 = a \cdot 0 + b \\
 \Downarrow b = 0
 \end{array}
 \begin{array}{l}
 \longrightarrow \\
 (3.5, 22) \\
 y = a \cdot x + 0 \\
 22 = a \cdot 3.5 \\
 a = 6.2857
 \end{array}
 \left. \vphantom{\begin{array}{l} (0,0) \\ y = a \cdot x + b \\ \Downarrow 0 = a \cdot 0 + b \\ \Downarrow b = 0 \end{array}} \right\} \Rightarrow y = 6.2857 \cdot x \Rightarrow \frac{y [\mu\text{m}]}{x [\text{min}]} = 6.2857$$

To make sure, however, that this is the right etch time, I will start out by etching three wafers with different time intervals. Then the etch rate can be calculated from these a bit more precise. As the project advances and new wafers are needed, they will all be depth measured, and the etch rate updated.

Wafer 1-3

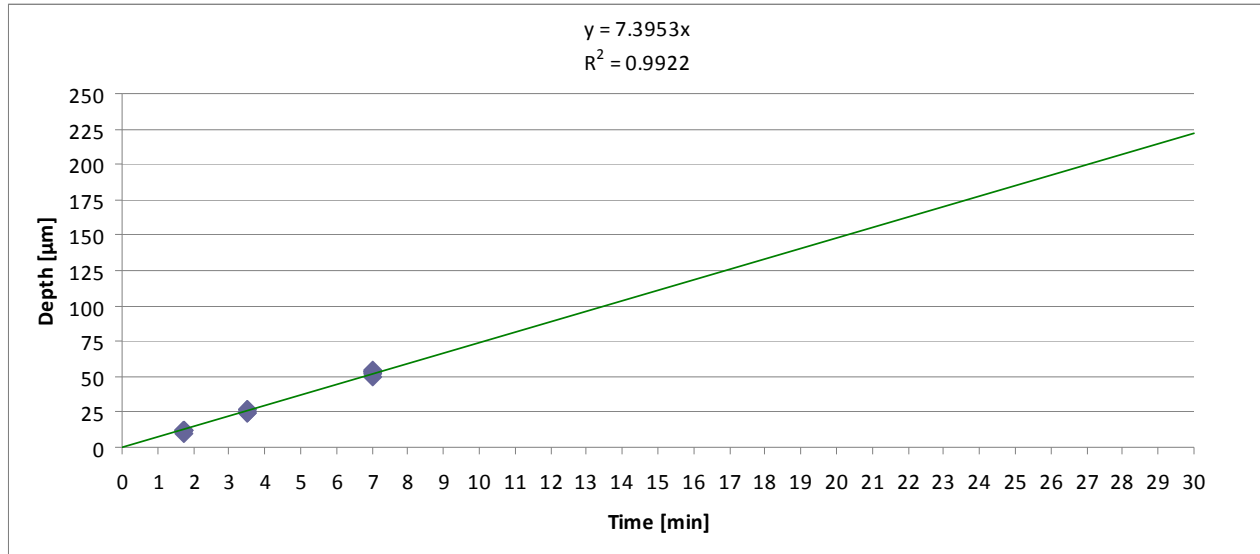
These wafers are all measured in the same places, and these places are all the 100 μm wide channels/platforms, which are the main areas that are going to be used:

Wafer no	Measuring place	Etch time [min]	Etch depth [μm]
1	Platform 100 μm east	3.5	25.41
1	Platform 100 μm (G4)	3.5	23.74
1	Channel 100 μm east	3.5	26.74
1	Channel 100 μm west	3.5	26.39
1	Platform 100 μm west	3.5	23.75
2	Platform 100 μm east	1.75	12.73
2	Platform 100 μm (G4)	1.75	12.38

Wafer no	Measuring place	Etch time [min]	Etch depth [μm]
2	Channel 100 μm east	1.75	10.03
2	Channel 100 μm west	1.75	12.37
2	Platform 100 μm west	1.75	12.27
3	Platform 100 μm east	7	49.84
3	Platform 100 μm (G4)	7	51.63
3	Channel 100 μm east	7	52.84
3	Channel 100 μm west	7	54.31



Plotting these numbers in a graph and adding a trend line crossing (0,0), we get:



The formula for the trend line is given and, hence the etch rate is:

$$y = 7.3953 \cdot x \quad \Rightarrow \quad \frac{y [\mu\text{m}]}{x [\text{min}]} = 7.3953$$

This etch rate can now be used to create wafers, with the desired platform depths.

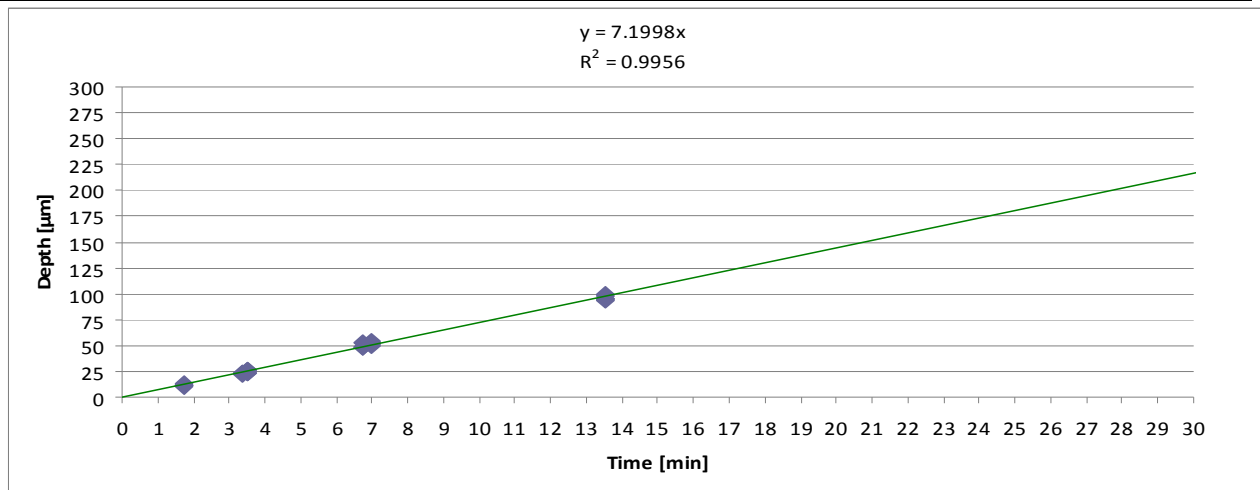
Wafer 1-7

These measurements are taken in the channels/platforms with the same width as the desired depth. This is again done, to have a step height fitting better for the areas going to be used rather than the whole wafer:

Wafer no	Measuring place	Etch time [min]	Etch depth [µm]
4	Channel 25 µm east	3.38	23.65
4	Platform 25 µm (G1)	3.38	21.52
4	Channel 25 µm west	3.38	23.85
6	Channel 50 µm east	6.76	48.18
6	Platform 50 µm (G2)	6.76	48.35
6	Channel 50 µm west	6.76	52.31

Wafer no	Measuring place	Etch time [min]	Etch depth [µm]
7	Channel 100 µm east	13.52	94.84
7	Platform 100 µm east	13.52	93.62
7	Platform 100 µm (G4)	13.52	95.43
7	Channel 100 µm west	13.52	99.86
7	Platform 100 µm west	13.52	97.89





Again the formula for the trend line is given and, hence the etch rate is:

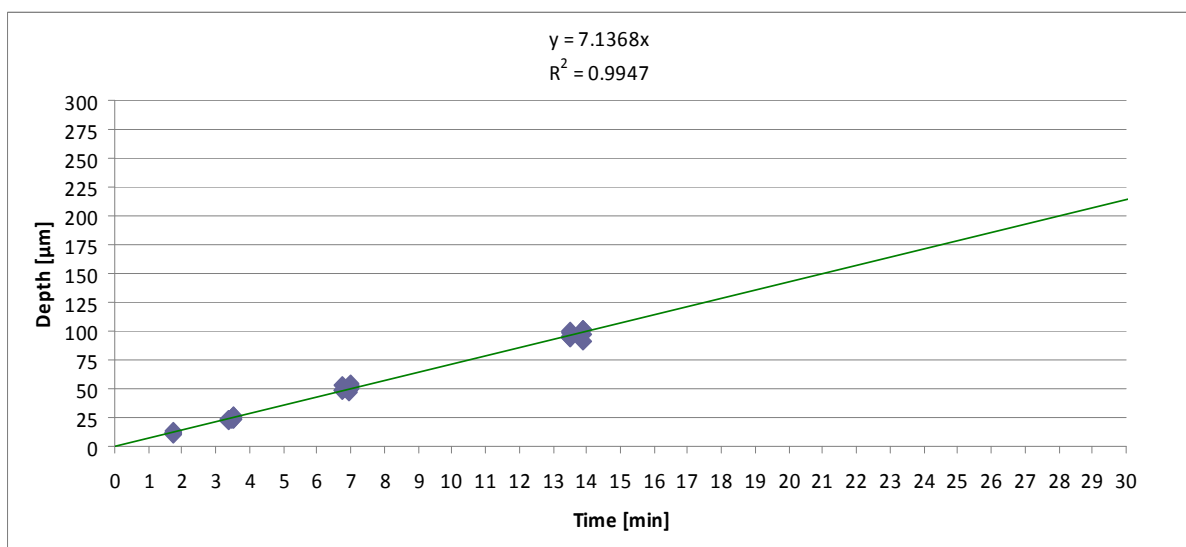
$$y = 7.1998 \cdot x \quad \Rightarrow \quad \frac{y [\mu\text{m}]}{x [\text{min}]} = 7.1998$$

Wafer 1-12

This time measurements are only taken in the channels/platforms that are going to be studied:

Wafer no	Measuring place	Etch time [min]	Etch depth [µm]
8	Platform 100 µm east	13.89	91.90
8	Platform 100 µm west	13.89	96.74
9	Platform 100 µm east	13.89	101.80
9	Platform 100 µm west	13.89	101.10
10	Channel 50 µm east	6.94	48.40

Wafer no	Measuring place	Etch time [min]	Etch depth [µm]
10	Platform 50 µm (G2)	6.94	47.48
10	Channel 100 µm west	6.94	50.35
11	Channel 25 µm east	3.47	23.77
11	Platform 25 µm (G1)	3.47	25.59
11	Channel 25 µm west	3.47	24.20



This time the etch rate given by the trend line is:

$$y = 7.1368 \cdot x \quad \Rightarrow \quad \frac{y [\mu\text{m}]}{x [\text{min}]} = 7.1368$$

If we look at the depth of wafer 8 and 9, which should be the same, we see a fairly large difference. Wafer 9 has almost the same depth for both measurements, whereas wafer 8 differs itself with around 5 μm . Compared to wafer 7 has wafer 8 and 9 been etched for 22 seconds longer, and should therefore be slightly deeper, which corresponds fine with wafer 9. For the hydrodynamic focusing purposes, a bit under etching of wafer 8, does not matter that much, since the focusing is done in the (x,y) direction and the depth just has to be large enough to allow 10 μm sized specimens to pass. Should a depth of 100 μm be crucial, adding a bit of over etch to the recipe (1-5 μm) can easily be done.

Selectivity between silicon wafer and photo resist

Now that the etching has been done the selectivity between etching the silicon wafer, and etching the photo resist on top, can be determined. This is done by calculating the etch rate for the resist. The resist thickness before etching was measured with the profilometer, and the thickness afterwards, is best measured in the SEM. Therefore a piece of the wafer has to be cut out before the resist is removed. Also this piece will be covered in a thin gold layer (25 nm), to make it more visible in the SEM. Because the resist is below 2 μm thick, the selectivity is calculated from one of the long ICP RIE runs (13 min 31 sec), to get the best result. The measurements are taken at the two 100 μm platforms:

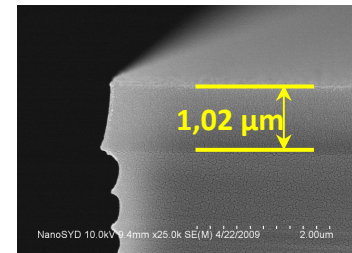


Figure 3.1.13: Resist thickness

Measuring place	Thickness before etch	Thickness after etch	Difference	Run time	Etch rate	Selectivity
Platform 100 μm east	1.64 μm	1.03 μm	0.61 μm	13.52 min	0.045 $\mu\text{m}/\text{min}$	1 : 160
Platform 100 μm west	1.55 μm	1.02 μm	0.53 μm	13.52 min	0.039 $\mu\text{m}/\text{min}$	1 : 184
Average	1.60 μm	1.03 μm	0.57 μm	13.52 min	0.042 $\mu\text{m}/\text{min}$	1 : 172

Because this photo resist etch rate is based on wafer 7, the silicon wafer etch rate is also taken from there, and it is calculated like this:

$$\frac{\text{Etch rate silicon}}{\text{Etch rate photo resist}} = \frac{7.1998}{0.0422} = 171.7 \quad \Rightarrow \quad (\text{photo resist}) \ 1 : 172 \ (\text{silicon})$$

So if we wanted to etch away all the photo resist, we would be able to etch silicon in the amount of:

$$171.7 \cdot 1.60 \mu\text{m} = 272.38 \mu\text{m}$$

The deepest desired silicon etch is 200 μm so this need should be covered, even if the calculations are off with more than 20 %.



3.1.10 Structure of the microchannels etched

After etching the first three wafers, a study of the channel structures is required to see if the etch is doing as supposed to. This will also be done in the SEM, once the resist has been stripped in acetone.

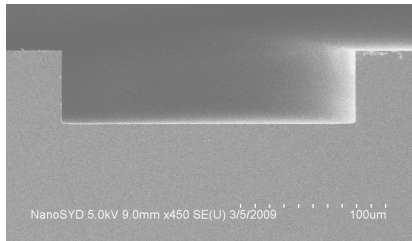


Figure 3.1.14: Wafer 3 profile

As we can see on figure 3.1.14, which is a picture of wafer 3, approximately 50 μm deep and 200 μm wide, the profile looks pretty good. A measurement of the angles gives for the left wall 89.7 degrees and for the right one 90 degrees, which is very good. The width is measured to be 202 μm and therefore also very precise. To make sure this is not a “lucky” picture, two other channels were examined and the results were equally fine. The angle was within 1

degree of being vertical and the widths of the channels were only off with a few micrometers. These minor errors can easily be caused by bad ruler placement, and also they all lie within the uncertainty of measurements.

3.1.11 Stripping the wafer for photo resist

All wafers are stripped after etching in the ICP RIE, to remove the used photo resist. It is done using acetone in a combination with the use of ultrasound. This is a fast way to remove the photo resist, however, it is fast drying and so some of the resist dissolved might reattach itself. Therefore quickly rinsing the wafers in water after stripping is important.

Stripping the wafer is for my project is important for when I want to use the SEM, since resist is not conductive and therefore would hinder a good image being made, and also for using the interference microscope, so that there is no refraction angle between the resist and the wafer, to give off false information.

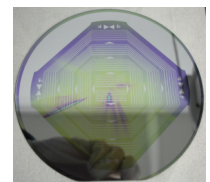


Figure 3.1.15: Wafer with resist



Figure 3.1.16: Wafer without resist

3.1.12 Breaking the wafer

To break the wafers into pieces that can be used, either as platforms or for studying, I use a little trick, where you carefully tap/scratch at the edge of a wafer with a hard tip (diamond or the like). Then at some point the wafer will break along its crystal structure, giving you a very clean cut. This is a good and fast method of cutting the wafers. There is always a chance when using this trick that you push too hard and break a chunk of the wafer instead of making a cut where you want. However as the pieces get smaller, they also cut easier.



Figure 3.1.17: Cutting of a wafer

After breaking the wafers into the desired platforms and channels, they are ready for sealing.

3.1.13 Hydrophobicity of the wafer surface

For the first batch (wafer 1-7) I did not finish the platforms by exposing them to oxygen plasma. However the second batch (wafer 8-12) were placed in a barrel etcher, and exposed to oxygen plasma. The plasma was sustained at 200 W with an oxygen flow of 200 sccm, for 2 minutes. This will remove any leftover resist from the wafers, and most importantly coat the wafers in a thin layer of silicon dioxide, which is hydrophilic.

To test the hydrophobicity both platforms are dipped in water and then pulled out [5.1.1.11]. If the surface is hydrophobic then most of the water will roll right off. If the surface is hydrophilic, the water should draw a wet line, trying to hold on to the platform:

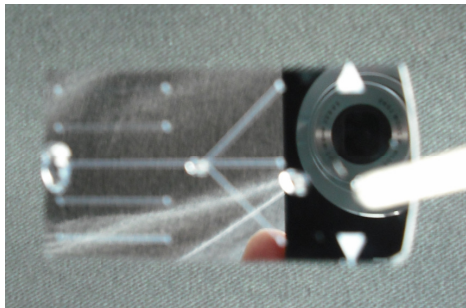


Figure 3.1.19:
Wafer 7 with not exposed to oxygen plasma

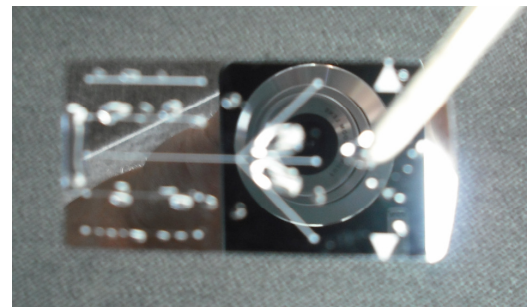


Figure 3.1.18:
Wafer 8 covered in silicon dioxide

As we can clearly see, the wafer that has not been exposed to oxygen plasma, is very hydrophobic. Whereas the wafer exposed to the plasma has been covered in silicon dioxide making it hydrophilic.

3.2 Platform assembly

After etching the channels and platforms in silicon, the platform should be assembled. Initially the four channels next to the platforms were connected with the same PDMS connector as the platform itself. At first this seemed like a good idea, making it possible to use both the channels and the platform for measurements. However it is hard to drill five holes in the PDMS with the correct distance between them. Also the smaller channels were

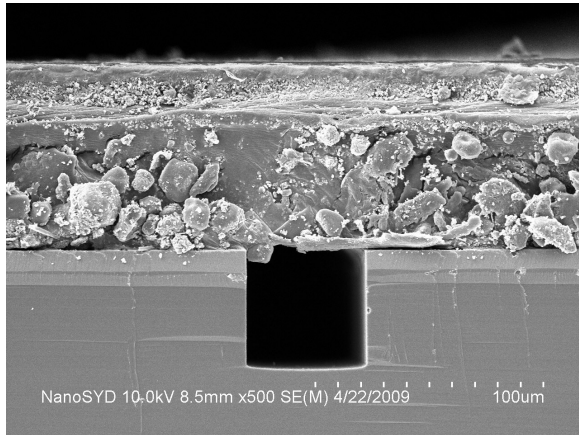


Figure 3.2.1:
Channel covered with an adhesive tape

hard to use without them pushing off the connectors, and in none of them could the liquid be pumped through. At first I thought this was because the adhesive layer of the tape (which is 25 μm thick) had been pushed into the channels, and so was clogging them. But by looking at cross-section of a taped channel in the SEM it was observed, that the tape is at most pushed only a few micrometers into the channels. Because a system covered with tape is hard to cut evenly, these pictures has been taken by breaking a silicon wafer containing micro-channels, and then placing the tape on top of it along this break. The tape's edges were even enough to make this alignment, so that no hand-cut "straight" lines were needed. However, the tape may not be pushed as far down into the channels at the edge than at the rest of the channel. Hence it is still hard to tell if the tape is blocking parts of the small channels. Also the output connectors for the channels are blocking any use of the microscope on the straight 100 μm platforms. Therefore further tests on the channels of sizes below 100 μm are forfeited until a working hydrodynamic focusing system is ready for the main 100 μm channels.

After a series of trial and error attempts made, trying to create non-leaking platforms, a procedure for minimizing the errors in the assembly process was found. This was done in collaboration with Stefan Johansen since he had a lot of the same issues trying to seal his PMMA channels. The procedure found, is however not perfected yet. Sometimes the tape will not stick to the platforms under operation, whilst at other systems it can withstand flow rates above 4000 μL/min (more than 16 times the operating flow). The cause of this error amongst others still needs to be investigated.

The procedure I have used with the most success is as follows:

3.2.1 Step 1: Apply adhesive tape

After the etched wafers have been oxidized for hydrophilic properties (and also to remove leftover resist and passivation), and have been cut into appropriate platform pieces, the adhesive tape is applied. By pulling the tape in one floating motion across the platform surface, a very fine surface can be achieved. Then using something with a very smooth edge (not too sharp though), the tape is pressed down onto the wafer whilst making sure there is



no air bubbles left. I normally use a piece of glass, which I cover with a clean piece of tape to soften the edge. If too many air bubbles get trapped under the sealing tape, it is pulled off and a new one is applied to avoid poor bonding between the tape and the silicon dioxide platform:

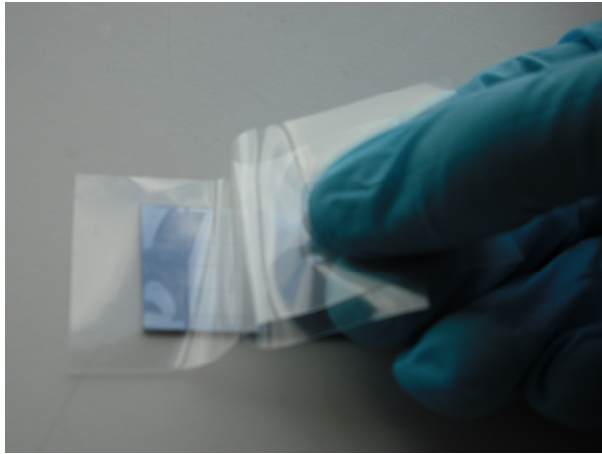


Figure 3.2.3: Tape being applied to a platform

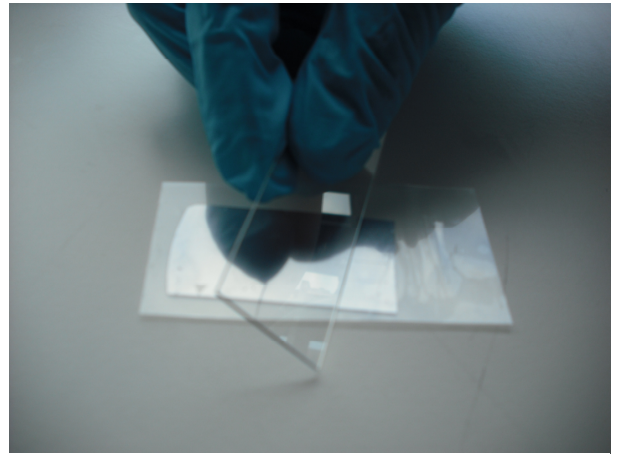


Figure 3.2.2: All air bobbles are removed

3.2.2 Step 2: Carve holes in the sealing for connectors

After the tape is applied, holes are cut in the sealing around the inlets, while taking care that the cut out pieces do not leave anything behind to block the flow afterwards:

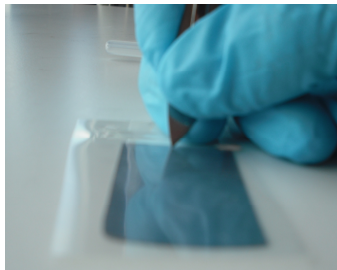


Figure 3.2.4:
Holes have to be cut at every inlet/outlet.

3.2.3 Step 3: Place the connectors

When all the holes have been carved, a needle is used to place connectors on top of the inlets. For the three input channels, connectors with holes fit for small hoses are placed. For the output channel, a connector is chosen with a larger hole, fit for the larger hoses. That way no unnecessary pressure is built up due to resistance in the exit hose:

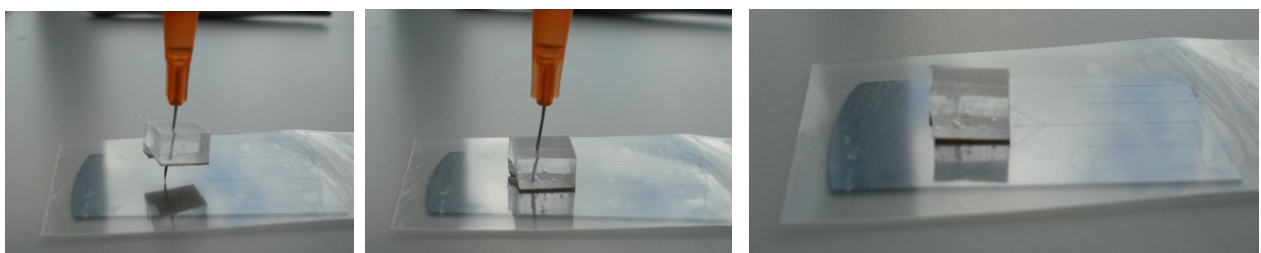


Figure 3.2.5: The needle is used to find the inlet/outlet. The then connector is glided down and attached.

3.2.4 Step 4: Apply cleaning vacuum

When drilling holes in PDMS, the material removed smoulders. Therefore there can easily be small dirt particles still sitting in the connector hole. When a hose is plugged in these dirt particles are pushed towards the channels. To get a minimum of dirt into the channel a vacuum is applied to each input connector, one at a time, using a spring by hand. The output connector should have room enough for these particles to leave the system when it is in use. Eventually demineralised water can be applied to the output connector during the vacuum step. This makes sure that there is a clear passage between input and output connectors, but it also help to clean out possible dirt particles.

3.2.5 Step 5: Water test



Figure 3.2.6:
Water is gentle pumped through to test if the connectors will hold

After the shortly exposing each channel to a little vacuum clean, it is time to test the connector's bonding. Using a syringe filled with water, this is pushed into each input channel one at a time, whilst the two unused input channels are connected through a little piece of hose. Pressure is then slowly applied until the water either comes out of the output connection, or between the filter paper and the double-sided adhesive tape. This turned out to be the weakest point in the system, and may be improved upon by using a filter paper with smaller pores the bond.

Approximately 1 out of 3-4 connectors are usually leaking. If a leak is observed then the leaking connector should be changed, following again step 3-5.

Step 6: Silicone sealing

After successful attaching the four connectors, silicone [5.1.1.12] is used to seal the connectors even better to the surface of the tape. This is then left night over to be sure it is hardened. If all goes well this procedure can make hydrodynamic focusing platform capable of withstanding a flow rate of over 4000 $\mu\text{L}/\text{min}$, even though this has not yet been tested for a very long duration time. When the flow rate is raised even further, it might happen that liquid begin to pour out between the hoses and connectors. To avoid that, the hoses can be sealed tight directly into the connectors using the same silicone as used on the bottom. This has not been tested though since I only had access to a very limited supply of thin hoses. Another method for creating stronger bonding between the hoses and connectors could also be to make the bonding holes using a needle instead of drilling. This make the PDMS cling more to the hoses.

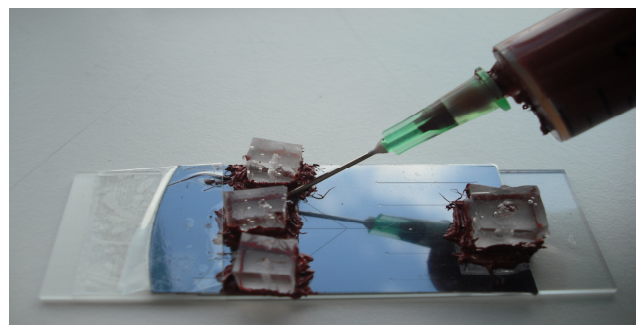


Figure 3.2.7: Sealing the connectors with silicone

4 Results and discussion from hydrodynamic focusing experiments

4.1 Hydrodynamic focusing

When measuring hydrodynamic flow focusing between two liquids, it can be very difficult to determine where to measure the focused width. Due to diffusion, the shape of the liquids flowing concurrently, shadows and more, it can be hard to draw thin lines between the liquids and measure the distance between them. Also the distance from the channel crossing and focus depth of the microscope used can alter the results greatly. To be able to obtain useful results, it is therefore important to measure the gathered data as uniform as possible. To help with that all images will be processed in the computer program SPIP [5.1.1.13]. This program has different tools to help collecting data from the gathered images. Also the pictures will be taken close to the channel crossing. I will now explain how I have gathered my data from the microscopy pictures using SPIP:

After an image has been imported a line is drawn across the area we wish to measure. This line can then be widened to average over a larger area. Averaging is used to avoid badly placed lines that may give straying results. A graph is drawn based on this averaging:

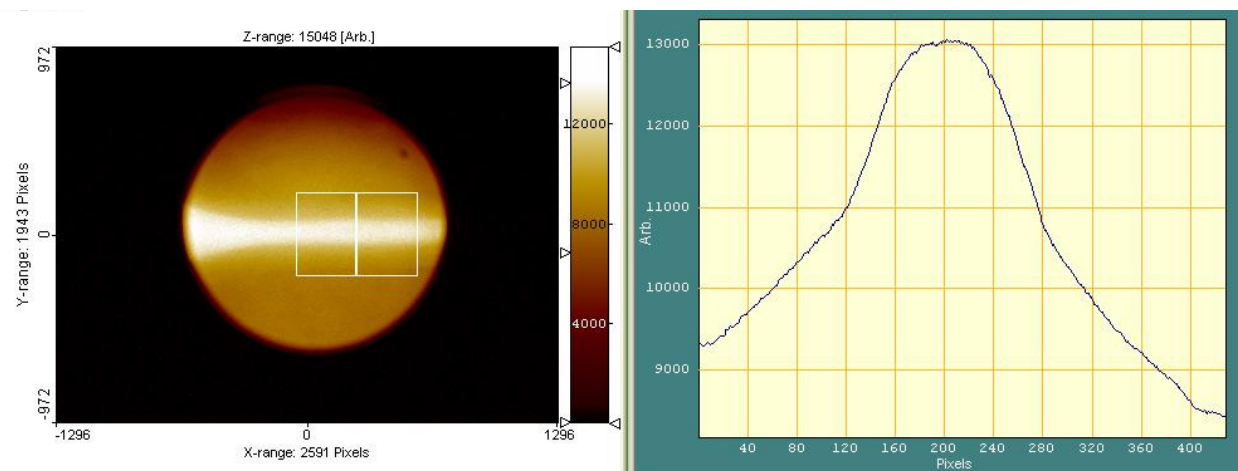
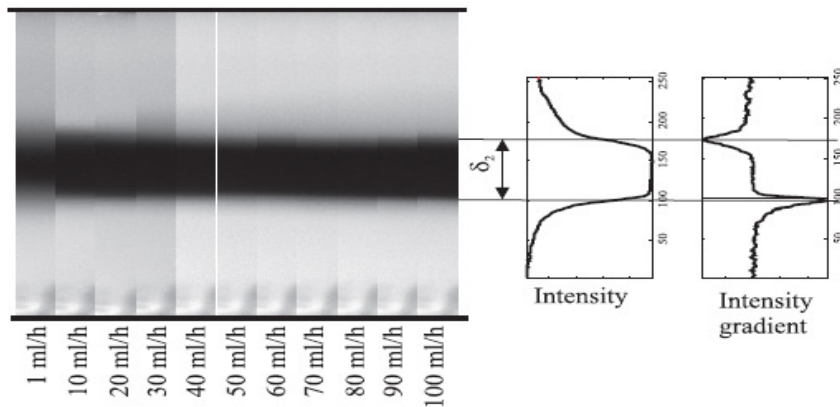


Figure 4.1.1: Averaging in SPIP

As can be seen it is difficult to determine where to measure the width of the focused flow on the graph, and make the exact same measure for all different channels. We can not count on the y-axis to tell us anything about the depth, since it is only based on the light intensity of the image, which does not correspond to the real depth. Therefore using the same y-value for all measurements will be invalid. Instead, however, we can differentiate the graph to get a picture of the gradients. These gradients will change direction, when shifting between sheaths flows to sample flow, making it easier to choose measurement uniform points. A good picture should give a graph looking like the one on the left [5.2.1.9]:



[5.2.1.9] Figure 4.1.2: Left picture is the intensity for different flows. Right is and almost ideal differentiated graph.

However, the pictures gathered for the various systems we have do not always give very steep curves. There is also usually a lot of noise due to small variations in the pictures light intensity. Therefore my pictures mostly look like this:

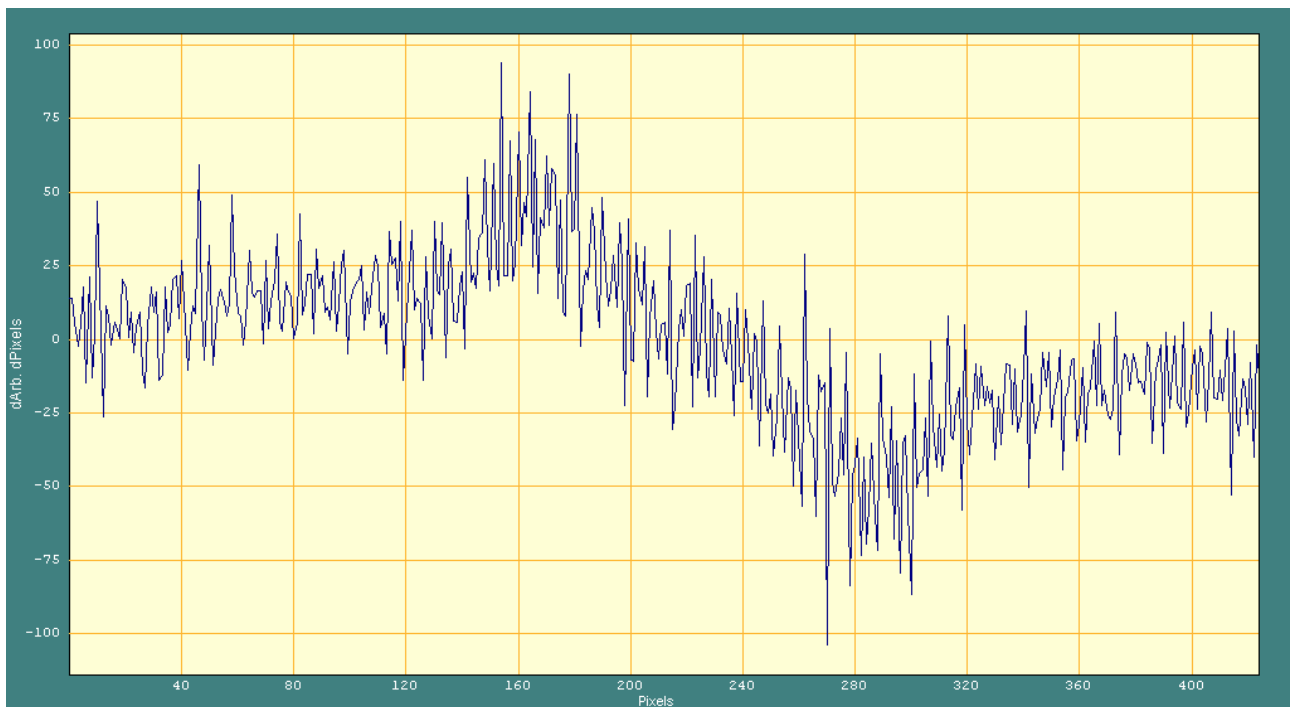


Figure 4.1.3: Noisy dy/dx graph.

And so it still can be hard to place measure markers in the same place every time, giving a uniform measurement. So to make it even clearer where to place measurement markers, the oscillating noise is removed by using a filter to smoothen the picture:



Figure 4.1.4: Smoothed dy/dx graph

However a smoothing of the picture may alter the graph and thereby shift the results creating false data. To find out how large an error this method is applying to the system, a range of pictures are made, using different magnitudes of filtering. Then they are compared to the unfiltered results, measured on both the differentiated graph, but also on the untampered average graph. The measurements are collected a few times for the same image to avoid large reading errors:

Measurements from averaged graph		
1st [px]	2nd [px]	Avg. [px]
372	371	371,5
372	371	371,5
373	371	372,0
		371,7

Measurements from dy/dx graph		
1st [px]	2nd [px]	Avg. [px]
371	374	372,5
372	374	373,0
372	376	374,0
		373,2

Kernel size (mean filter)	Measurements from smoothed dy/dx graph		
	1st [px]	2nd [px]	Avg. [px]
3	372	376	374,0
5	372	375	373,5
7	373	374	373,5
9	372	373	372,5
11	372	372	372,0
13	374	371	372,5
15	373	371	372,0
25	372	371	371,5
35	373	371	372,0
55	373	368	370,5
			372,4

As can be seen the averaged graph average is ≈ 372 pixels. This measurement is very reliable. The measurements made on the unfiltered differentiated graph, is also close to this number – especially all the first points. All the smoothing done seem to have had no negative effect on the unfiltered data. Only when a filter of a very high number is applied do larger variations appear. Based on these observations, smoothing with a kernel size of 11 is chosen. This was the only measurement in which we have been able to choose the exact two points



for measure. Also the result is 372 pixels, which fits with both the smoothed average, but also the averaged average. Henceforth all pictures will be smoothed before comparison, to make sure the right gradient is chosen.

4.1.1 Image gathering

To help deciding which microscope to use for gathering all the images (the fluorescent or the Navitar setup), looking at the magnifications of the microscopes is a good place to start, since I need to be able to measure differences in the flow width of 1 μm in size. On the fluorescence microscope objectives giving: 5, 10, 25, 50 or 100 times magnification can be chosen. However, because the lid between the focused flow and the objective is too thick, the 100x objective is unable to focus in the correct depth. For the Navitar setup we have only a 20x objective, but here it is combined with a zoom lens system capable of magnifying the view another 6.5 times, giving a total magnification of 130x.

This is only true though, if the cameras internal magnification is 1. Since two different cameras are used in the microscopes, there might be a difference in this magnification. To find out I simply make a test picture with both cameras of something with a known size, set the same resolution for both pictures, and then measure the real scale differences:

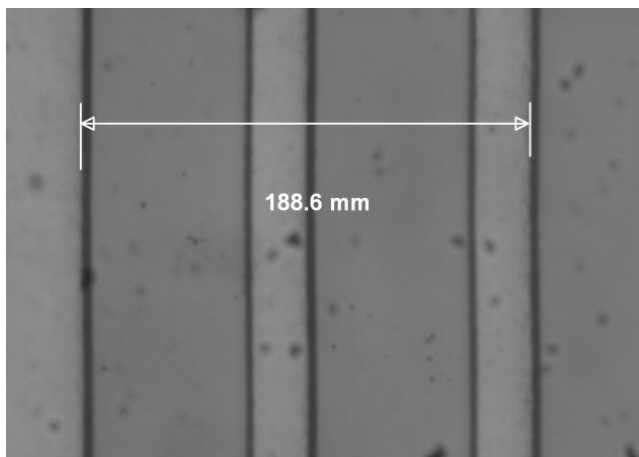


Figure 4.1.6: Navitar setup

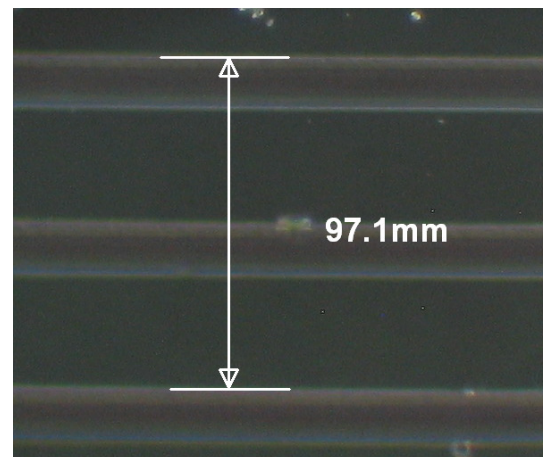


Figure 4.1.5 : Fluorescence microscope

The distance measured is 100 μm wide. Hence the magnification for the two pictures is:

$$188600\mu\text{m} : 100\mu\text{m} \Rightarrow 1886:1$$

$$97100\mu\text{m} : 100\mu\text{m} \Rightarrow 971:1$$

This gives a relation of:

$$1886:971 \Rightarrow (\text{Navitar}) 1.94:1 (\text{Fluorescence})$$

Hence I was going to use the Navitar setup to take the pictures, since it can take pictures giving almost twice the resolution, and thereby more points are used for calculating the average width, which gives a better result. However it turned out to be difficult to gather



data with the Navitar setup, because general vibrations present in the working laboratory, created waves on the images:

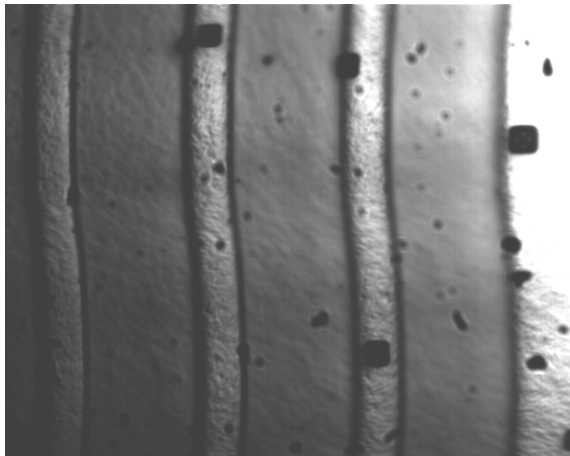


Figure 4.1.8:
Wave shaped distortion created by environment

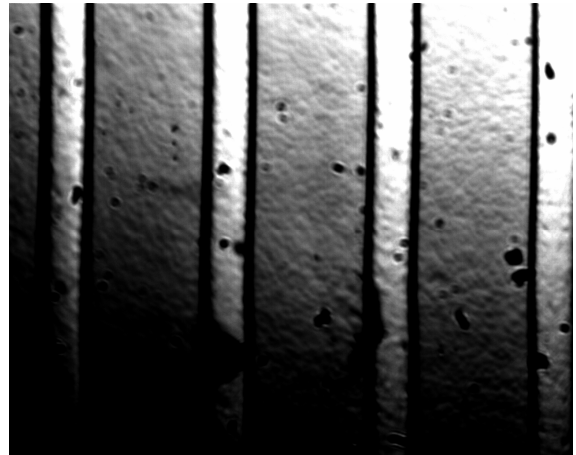


Figure 4.1.7:
Poor lighting resulting in uneven shadowing

Also the lighting applied was not 100 % from the top, resulting in shadows that changes the channel width in one side. Using two lamps, or attaching a lamp so that is shines onto a semi transparent mirror, illuminating the sample from above, this error could greatly be reduced.

Lastly the results gathered were hard to extract from the images. Bad lighting causes too many light intensity changes in the channel making even the smoothed graphs hard to interpret:

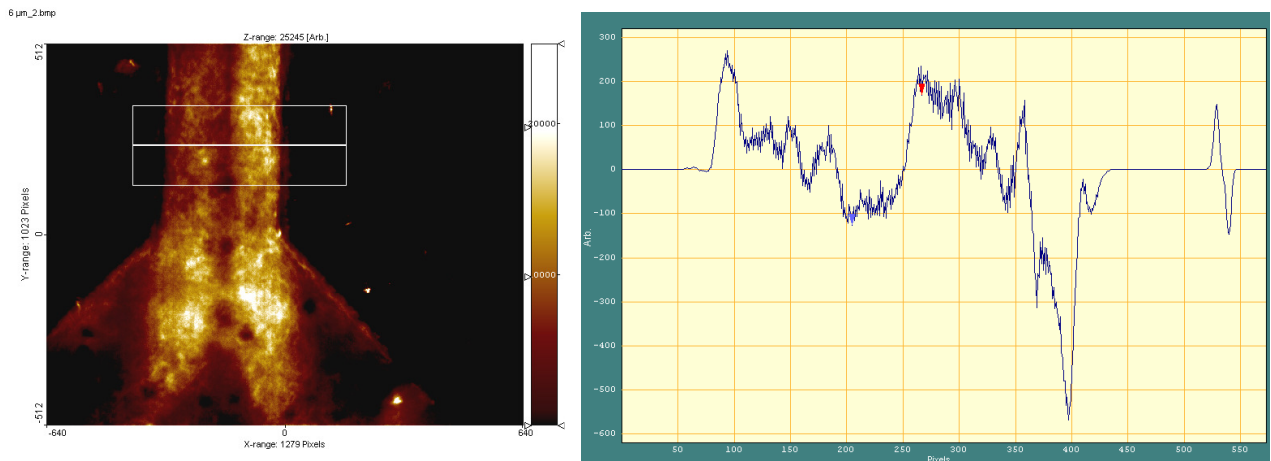


Figure 4.1.9: Image in SPIP taken with Navitar setup

So after one full measurement of wafer 7 (see Navitar microscope below), it was decided to use the fluorescence microscope instead.

4.1.2 Calibration measurements

All pictures gathered and processed in SPIP results in the channel widths being represented in pixel. To calculate how much this responds to in micrometers a known length needs to be measured, and then the pixel/ μm ratio can be determined. The known length used, is a little chip we got from supervisor Jakob Kjelstrup-Hansen which has hills $35 \mu\text{m}$ wide separated with $15 \mu\text{m}$ gaps (see figure 4.1.10). So by measuring a distance of two hills and two gaps, the number of pixels represented by SPIP for this length will be equal to $100 \mu\text{m}$. An image will be taken, of the chip used for calibration, for both the Navitar setup and the fluorescence microscope, to make sure the right ratios apply for the right microscopes. The ratios gathered are:

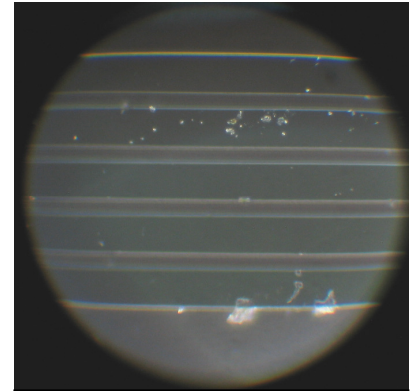


Figure 4.1.10: Calibration chip

	No. of pixels measured	Ratio	
		pixel	μm
Navitar setup	367	3.67	1
Fluorescence microscope	372	3.72	1

4.1.3 Mutual performance comparison of platforms

To have a basis for comparing the commercial platform, with my silicon platforms, and Stefan Johansen's PMMA platforms, we decided to make a common list to be used for measuring the samples. Because one of the aims of this project is to end up with focused flows of a certain size, the list is a set of numbers, which corresponds to the theoretical focused flow widths, we would like to measure in the end. However, the pumps used to achieve these widths, are controlling the channel flow, and therefore the associated sample flow is calculated using equation (1):

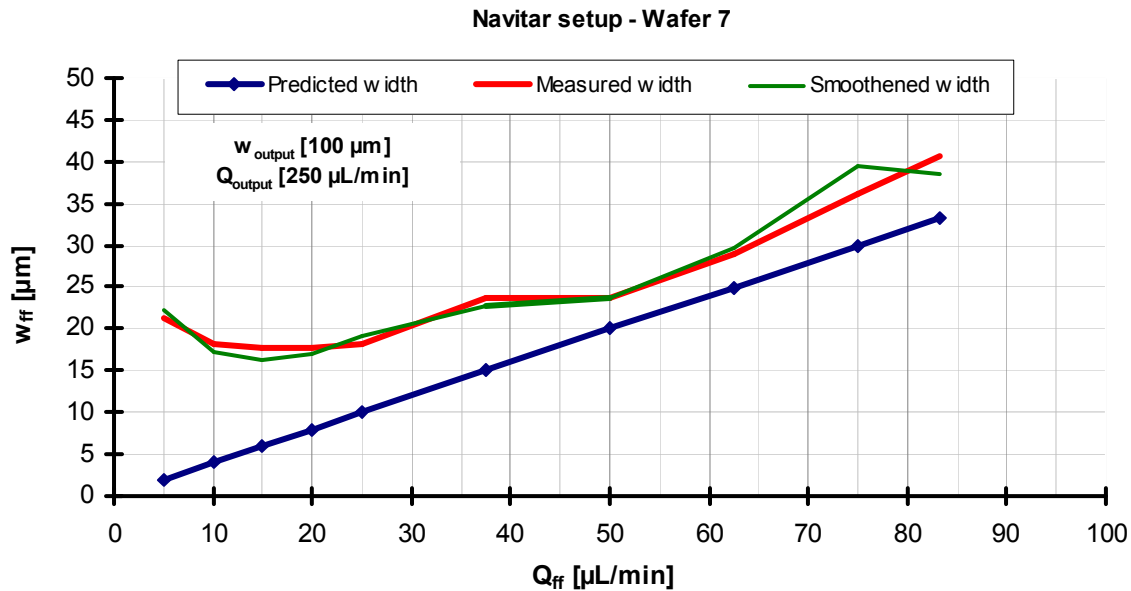
Theoretical focused flow width	Flow for the $100 \mu\text{m}$ silicon system's sample channel
$w_{ff} [\mu\text{m}]$	$Q_{\text{sample}} [\mu\text{L}/\text{min}]$
2	5
4	10
6	15
8	20
10	25
15	37.5
20	50
25	62.5
30	75
1/3 of channel width	83.3



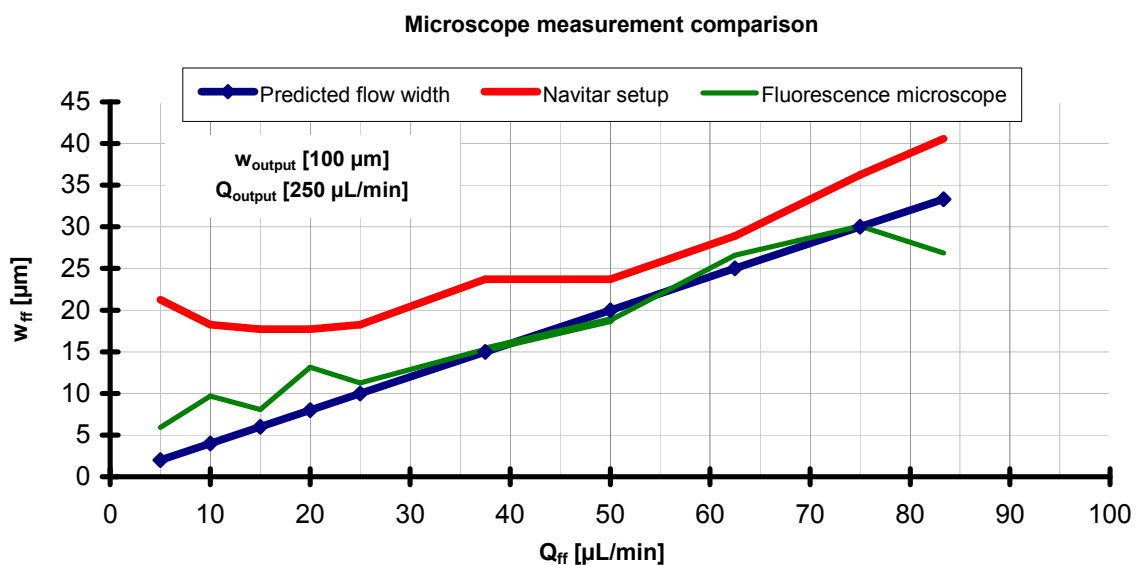
Figure 4.1.11: Fluorescent microscope setup

4.1.4 Navitar microscope

Before switching to use the fluorescence microscope, wafer 7 was measured on the Navitar setup. By plotting the focused flow and comparing it to the focused width, a comparison can be made with the measured numbers:



The smoothed and the non-smoothed curve are very much alike, with exception of the last two readings. Both curves start out with a channel width more than twice the expected size, and first around a width of 25 μm , do we get within 5 μm of the desired value. Normally this difference means that the focussed flow is wider than expected. However, in case of the Navitar system this large deviation might be caused by to many sources of errors, like bad lighting. This can be seen if we compare the measurements with the ones made on the fluorescence microscope:



The pictures from the fluorescence microscope appear much close to the theoretical curve than the ones from the Navitar. This was expected because of the poor lighting I used in the Navitar setup. The Navitar setup is namely still under construction with adjustments pending. Furthermore it is built to detect fluorescent beads using laser light, in the detection phase of cytometry, and not for hydrodynamic focusing.

4.1.5 Fluorescence microscope

Early in the project was the commercial system's possibility for hydrodynamic focusing tested using the fluorescence microscope. At the time we had no standardized foundation for measuring, so before measuring my own systems and also Stefan Johansen's systems, the commercial system is measured again:

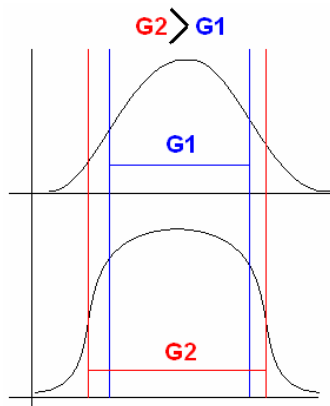
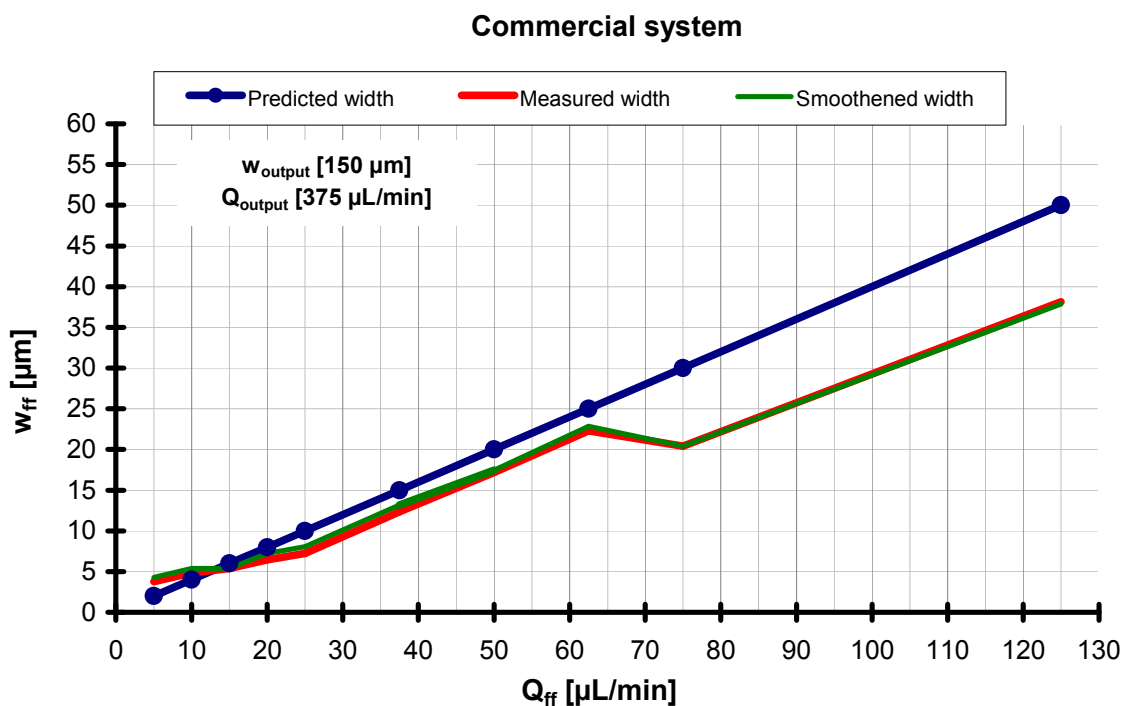
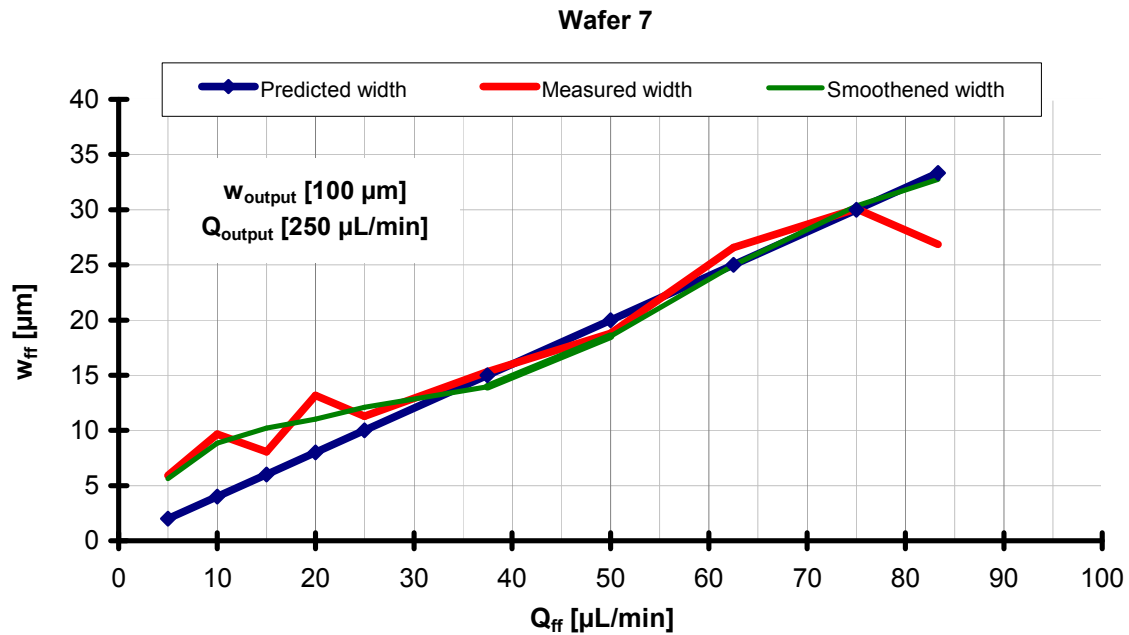
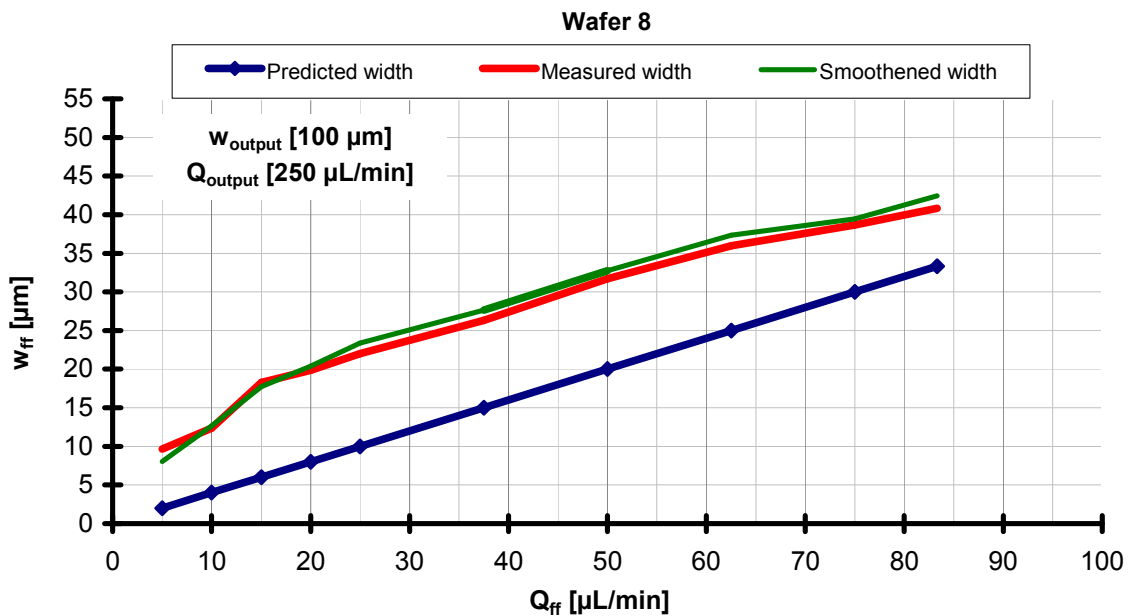


Figure 4.1.12: Comparison of different intensity curves

The commercial systems measured flow and smoothing, fit very well together. Until the flow exceeds 62.5 μL/min, they match the theoretical flow within a 3 μm margin. This is still too much of a change in size at the lower end, where such a change can be three times as wide as supposed. Above a flow of 62.5 μL/min the difference increases to around 10 μm. Looking at the raw images used for measuring these last to points, I notice that they are less intense in the color of the focused channel. Since an intense curve will have a sharper and more distinct edge and therefore a less pointed curve than a dim curve (see figure 4.1.12), this should make the last to points become wider than the rest with about approximately 1-2 μm. Instead they are narrower by a factor far larger, and so I can only speculate to why this error happens, like maybe the objective focus has accidental been shifted during measurement.

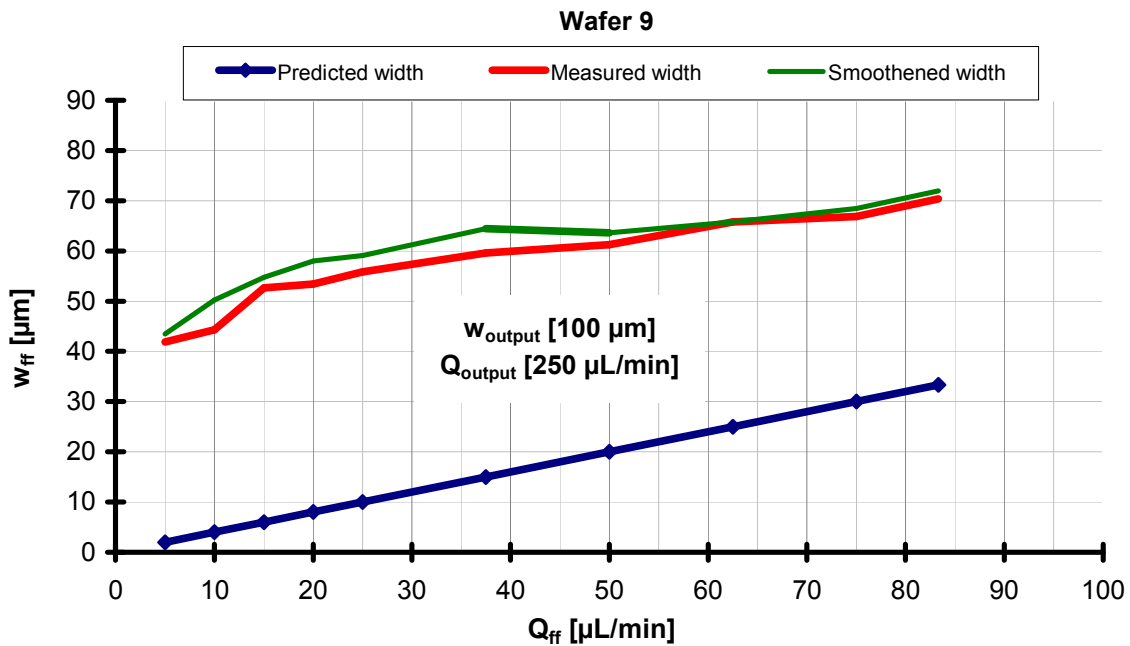


Next I look at my silicon platforms. The measured curve for Wafer 7 as above is “jumping” a bit in both ends of the curve, whereas the smoothed image is more even and follows the theoretical curve nicely, above a focused flow width of 10-12 μm . Below that value it is wider than estimated, and it is also in this area the measured curve “jumps”.

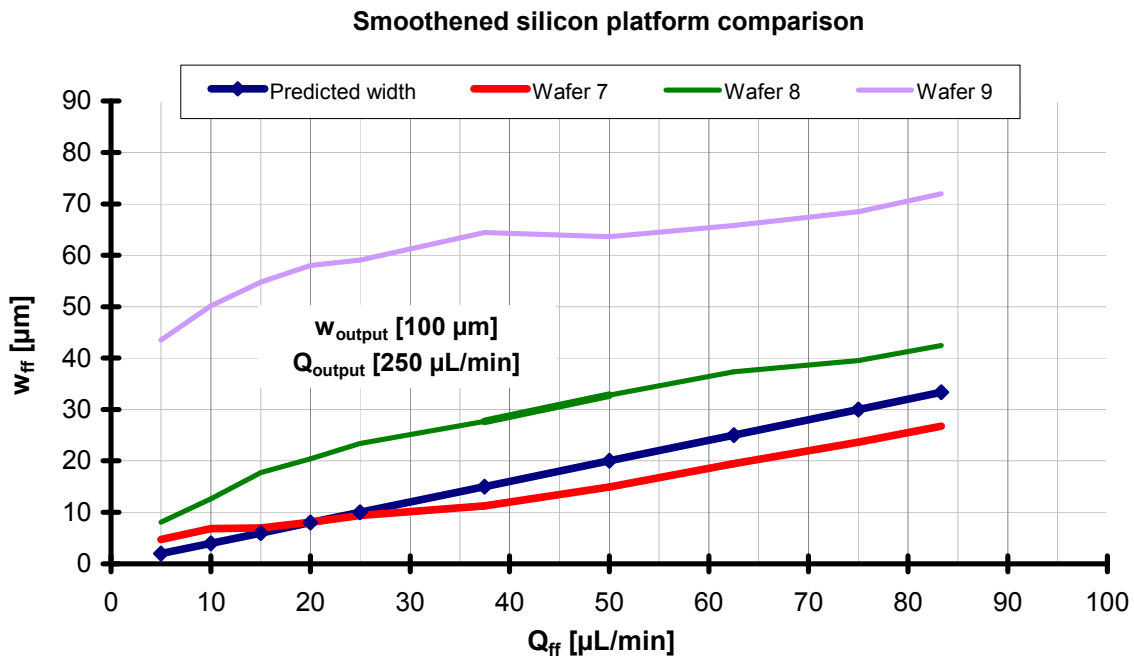


For silicon platform 8 shown in the graph above, there is again a good correspondence between the measured and the smoothed curve, but this time they are shifted approximately 10 μm above the theoretical curve.



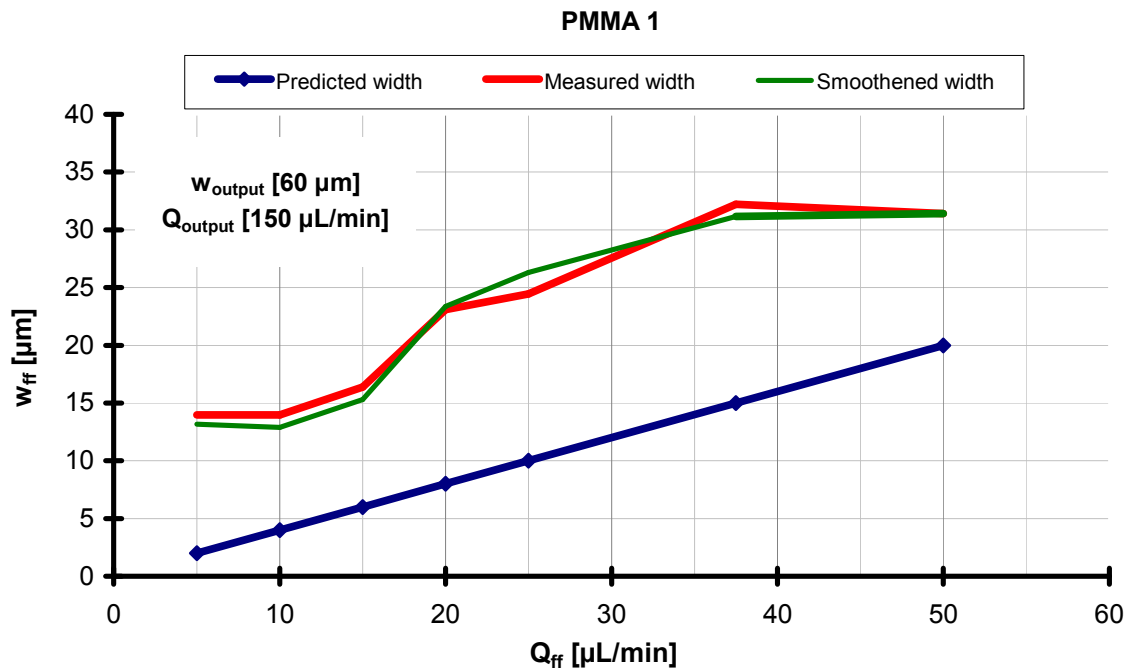


The measurement and smoothing curves valid for the graph above, are in range of 3 μm apart, even though they follow a similar pattern. They are also both about 40 μm of scale from the theoretical curve. However, these pictures are all out of focus and this is what probably causes the very large shift. I was going to take the pictures all over, but after the first revised image liquid started to lift of the lid, rendering my platform useless.

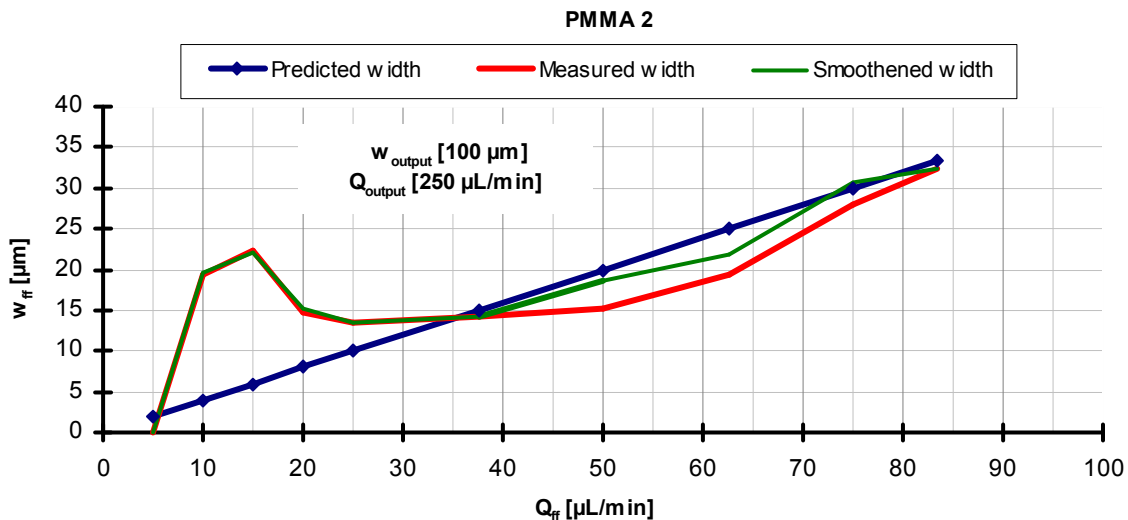


If comparing the three systems I managed to fabricate and test, then we can see that the platform made from wafer 8 and 9, follows a very similar pattern, even though platform 9, has been widened due to a poor focus of the microscope. Other than that are all the curves quite straight with approximately the same gradient.



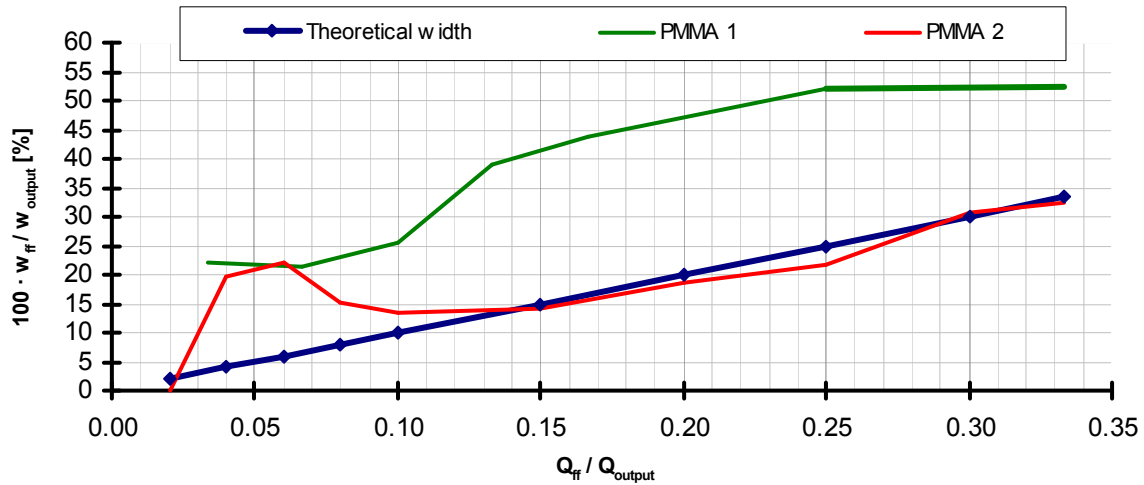


The graph above shows the first PMMA platform that worked. It is not as straight as the silicon platforms but it does seem to revolve about a similar line offset by approximately 10-15 μm from the theoretical curve. The measurements have only been made for flows up to 50 μL/min in the sample channel. After that the pressure became too big, at the sample inlet, creating a leak. The measured and smoothed curves fit within 1 μm at the smaller critical places, and within 2 μm for the flow at 25 μL/min.



The measured and smoothed curves on the above figure are very close together from 5 to 37.5 μL/min. Then the two curves part with around 3 μm in difference until they combine again at 83.3 μL/min. In the first part the measured and smoothed flow start far from the theoretical flow (first value plotted is zero and thus are forfeited), and then descent until close to the theoretic curve. From there on the smoothed flow follows the theoretical flow varying up to 3 μm. The measured is a bit more of with around 6 μm.

Smoothened PMMA platform comparison

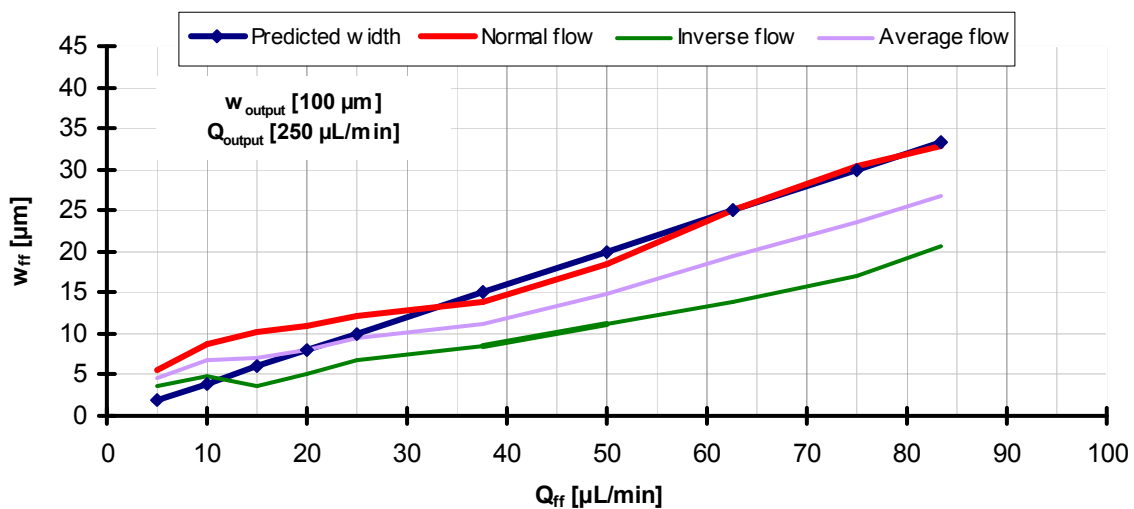


The combined PMMA plot in the graph above, show almost inverted behavior between the to platform sizes with the one taking up around 25% more space. In the lower end of PMMA 2 is the distance to the theoretical curve largest. When the focused flow becomes small, it is hard to measure the correct values. This would explain why the PMMA 2 curve gets closer to the theoretical curve when the flow ratio gets larger. The difference is at first 19 % off. Now since all channels in the PMMA 1 are only around half the size of the ones in PMMA 2, it might be mean that it is also approximately twice as hard to gather the correct data. A 25 % overshoot is not much more than the 19 % for PMMA 2.

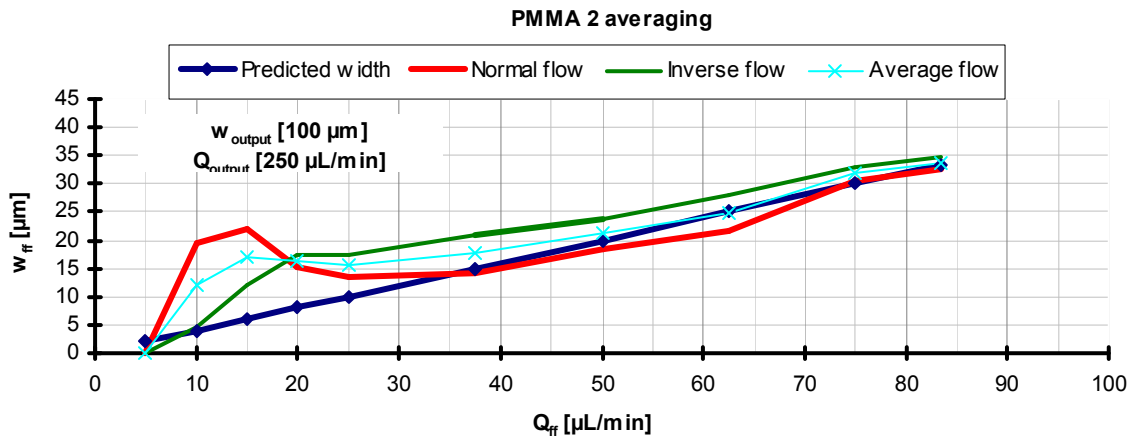
4.1.6 Averaging flow measurements

Because there might be diffusion of scattered light that makes the focused flow in the output channel appear wider, a measurement of the inverted process is made. Here we ad the dye to the sheath flows and then focus demineralized water. That way if there is a diffusion or lightning error it will show. For the silicon platform 7 this gives:

Wafer 7 averaging



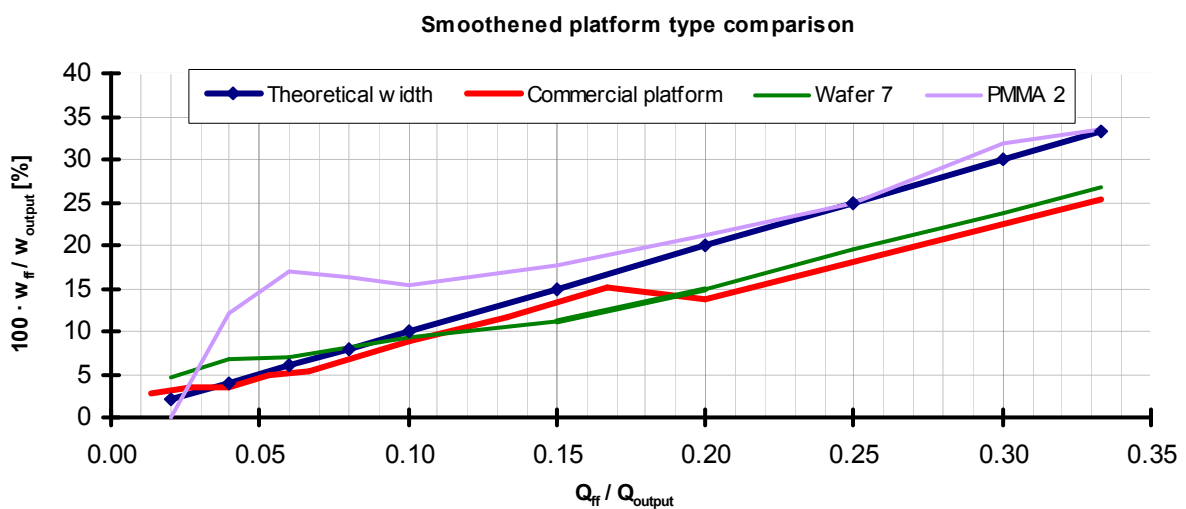
As shown the inverted curve is actually narrower than for the normal flow. In order for the average curve to fit onto the theoretical, both the normal and the inverse curve must have a wider focused flow. However, some of the other systems (fx platform 8) had a curve placed above the theoretical one. So if the inverse readings where to be taken from this one, then the average curve might be placed very close to the theoretical one. This is not possible to do though, since the wafer broke during a needed tape change. So in order to fully test this theory for my silicon systems, new wafers need to be made. Instead the same test is being made for the PMMA 2 system, so this will also be examined:



As we can see on this graph, is the average curve the one that fits the theoretical curve the best. So henceforth all measurements made, should be made for both the normal and the inverse system. At least until enough data is present to estimate the normal curves overshoot. Then multiplying the focused flow width with this estimate may give a useful curve. Since the flow width in the important area (1-10 μm) has not been successfully measured on any of these systems, this needs to be worked out, before applying a method that can easily be yet another source of error.

4.1.7 Platform type comparison

Lastly a comparison of the different types of systems is done:



Here it seems that the different systems have a favored working area. The PMMS is not good for small flow ratios, but may be used with success in larger systems. The commercial system works the best in the small flow ratio area, and worst at ratios above 19. Therefore these systems may be the best to use for the larger cytometry project where the small scale focusing is needed. In general the silicon platforms are a bit more off target than the other systems in their working areas. However, it has a more steady distribution along the whole scale, so this might be a good solution for systems that need a variety of focusing.

When all this is said I must also strongly point out that these measurements are based on a few systems measured only once. If any validity should apply to these conclusions, then a lot more testing needs to be done and this must then show the same as the graphs used in this chapter.

4.1.8 Sources of error

First of all, when collecting data from the images, the pictures should be good enough for the same numbers to be collected from the same picture by two different people. For a lot of our data we had trouble recollecting them, and therefore it might be an idea to have a larger picture resolution, giving more details about the small focused flows. When using smoothed readings, the readings should not change more than 1-3 pixels which are about the same as 1 μm .

Also, when applying only low flow rates in the beginning of a test, air bobbles tend to get stuck in the crossing area. Increasing the flow whilst tapping gently on the input hoses, and applying a vacuum (using a syringe) on the output may help to remove these bubbles. Flow focusing sometimes still happen, with the sample flow being directed around the bubbles before sampling. However this can cause the focused flow to be closer to one side than the other.

Diffusion or reflecting fluorescent light may be the cause of the widened focused flows in the channels. However, the simplified equations used to calculate the focused flow width might also be incorrect.



5 List of references

5.1 Internet

5.1.1 Websites

- [5.1.1.1] <http://www.chem.agilent.com/en-us/products/instruments/lab-on-a-chip/2100bioanalyzer/cellsolutions/pages/default.aspx>
- [5.1.1.2] <http://www.interreg4a.dk/wm242732>
- [5.1.1.3] http://www.engineersedge.com/fluid_flow/flow_velocity_profiles.htm
- [5.1.1.4] http://www.oxfordplasma.de/technols/rie_remo.htm
- [5.1.1.5] http://www.rsc.org/Publishing/Journals/lc/PDMS_connector.asp
- [5.1.1.6] <http://www.whatman.com/QuantitativeFilterPapersAshlessGrades.aspx>
- [5.1.1.7] <http://www.dowcorning.com/applications/search/products/Details.aspx?prod=01064291&type=PROD>
- [5.1.1.8] http://www.harvardapparatus.com/webapp/wcs/stores/servlet/product_11051_10001_44012_-1_HAI_ProductDetail_37315_____
- [5.1.1.9] <http://groups.mrl.uiuc.edu/dvh/pdf/AZ5214E.pdf>
- [5.1.1.10] http://www.first.ethz.ch/infrastructure/Chemicals/Photolithography/Data_AZ351B.pdf
- [5.1.1.11] http://www.microlab.ucla.edu/ResourcesLinks/process_info.htm
- [5.1.1.12] http://www.wurth.com.au/msds/o890_321.htm
- [5.1.1.13] <http://www.imagemet.com/index.php>

5.1.2 Wikipedia.org

- [5.1.2.1] <http://en.wikipedia.org/wiki/Pmma>
- [5.1.2.2] http://en.wikipedia.org/wiki/Reynolds_number
- [5.1.2.3] <http://en.wikipedia.org/wiki/Viscosity>
- [5.1.2.4] [http://en.wikipedia.org/wiki/Water_\(molecule\)#Density_of_water_and_ice](http://en.wikipedia.org/wiki/Water_(molecule)#Density_of_water_and_ice)
- [5.1.2.5] <http://en.wikipedia.org/wiki/Laminar>
- [5.1.2.6] http://en.wikipedia.org/wiki/Contact_angle
- [5.1.2.7] <http://en.wikipedia.org/wiki/Hydrophilic>
- [5.1.2.8] <http://en.wikipedia.org/wiki/Hydrophobe>
- [5.1.2.9] <http://en.wikipedia.org/wiki/Polydimethylsiloxane>
- [5.1.2.10] <http://en.wikipedia.org/wiki/Eosin>
- [5.1.2.11] http://en.wikipedia.org/wiki/Trypan_blue
- [5.1.2.12] [http://en.wikipedia.org/wiki/Bis\(trimethylsilyl\)amine](http://en.wikipedia.org/wiki/Bis(trimethylsilyl)amine)
- [5.1.2.13] <http://en.wikipedia.org/wiki/Photolithography>



5.2 Bibliography

5.2.1 Articles

- [5.2.1.1] Microfluidics for flow cytometric analysis of cells and particles
by Dongeun Huh, WeiGu, Yoko Kamotani, James B Grotberg and Shuichi Takayama
Received 17 August 2004, accepted for publication 6 December 2004
Published 1 February 2005
- [5.2.1.2] Some useful yield estimates for ion beam sputtering and ion plating at low bombarding energies
by P. C. Zalm
Received 29 August 1983; accepted 5 January 1984
- [5.2.1.3] Measurements of scattered light on a microchip flow cytometer
with integrated polymer based optical elements
by Z. Wang, J. El-Ali, M. Engelund, T. Gotsæd, I. R. Perch-Nielsen,
K. B. Mogensen, D. Snakenborg, J. P. Kutter and A. Wolff
Received 15th January 2004, Accepted 17th March 2004
First published as an Advance Article on the web 20th April 2004
- [5.2.1.4] Plasma etching—A discussion of mechanisms
by J. W. Coburn and Harold F. Winters
J. Vac. Sci. Technol. Volume 16, Issue 2, pp. 391-403 (March 1979)
- [5.2.1.5] Deep Reactive Ion Etch Conditioning Recipe
by Matthew Wasilik, Ning Chen
Berkeley Sensor & Actuator Center
- [5.2.1.6] A Kinetic Model for Plasma Etching Silicon in a SF₆/O₂ RF Discharge
by H. M. ANDERSON, J. A. MERSON, AND R. W. LIGHT
IEEE TRANSACTIONS ON PLASMA SCIENCE, VOL. PS-14, NO. 2, APRIL 1986
- [5.2.1.7] Determining the optimal PDMS–PDMS bonding technique for microfluidic devices
by Mark A Eddings, Michael A Johnson and Bruce K Gale
Received 15 January 2008, in final form 6 March 2008
Published 25 April 2008
- [5.2.1.8] Hydrodynamic focusing for vacuum-pumped microfluidics
by T. Stiles Æ R. Fallon Æ T. Vestad Æ J. Oakey
D. W. M. Marr Æ J. Squier Æ R. Jimenez
Received: 3 November 2004, accepted: 10 December 2004
Published online: 31 March 2005
- [5.2.1.9] Microfluidic rheometer based on hydrodynamic focusing
by Nam-Trung Nguyen, Yit-Fatt Yap and Agung Sumargo
Received 14 April 2008, in final form 11 May 2008
Published 30 June 2008
- [5.2.1.10] Focusing Fluids and Light
by Xiaole Mao and Tony Jun Huang
IEEE Nanotechnology Magazine, March 2008



5.2.2 Books and pamphlets

- [5.2.2.1] Microsystem design Chapter 13: Fluids
by Stephen D. Senturia
ISBN 0-7923-7246-8
- [5.2.2.2] Introduction to Micro Fabrication Chapter 11: Etching
by Sami Franssila
ISBN 0-470-85106-6
- [5.2.2.3] Principles of Plasma Discharges and Materials Processing Chapter 15: Etching
by Michael A. Lieberman and Allan J. Lichtenberg Chapter 9: Chemical, kinetics and
ISBN 0-471-72001-1 surface properties
- [5.2.2.4] Silicon VLSI Technology: Fundamentals, Practice, and Modeling Chapter 9: Thin film deposition
by James D. Plummer, Michael D. Deal, Peter B. Griffin Chapter 10: Etching
ISBN 0130850373
- [5.2.2.5] Inductively Coupled Plasma Etching for Microsystems
by Søren Jensen
MIC - Department of Micro- and Nanotechnology,
Technical University of Denmark
- [5.2.2.6] Microscopy from the very beginning
Produced by Zeiss
Author Dr. H. G. Kapitza
2nd revised edition



6 Appendix

6.1 My attachments

6.1.1 Reynolds number

The Reynolds number is calculated using the following formula found in wikipedia [5.1.2.2]:

$$Re = \frac{\rho \cdot V \cdot D}{\mu} = \frac{V \cdot D}{\nu} = \frac{Q \cdot D}{\nu \cdot A}$$

Where:

Re is the Reynolds number

V is the mean fluid velocity [m / s]

D is the diameter [m]

η is the dynamic viscosity of the fluid [Pa · s]

ν is the kinematic viscosity [m² / s]

ρ is the density of the fluid [kg / m³]

Q is the volumetric flow rate [m³ / s]

A is the cross-sectional area [m²]

However, since the channels I have are square, D can for rectangular ducts be found using the following equation:

$$D_{\text{Rectangular}} = \frac{4 \cdot A}{P}$$

Where:

P is the wetted perimeter [m]

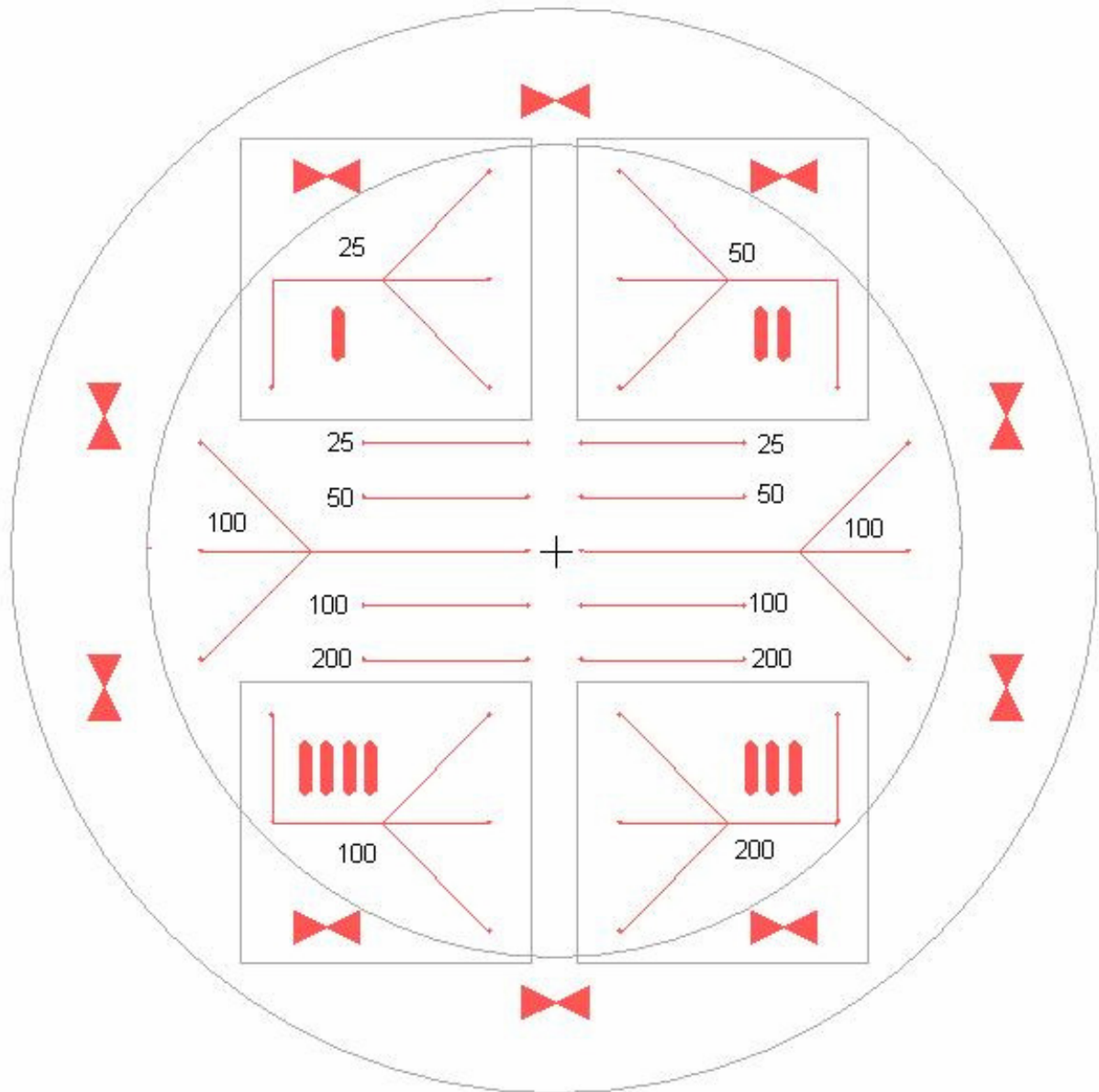
My mask design is made for channels 100 μm in both depth and width giving the following:

Parameter	Math operation	Result	Unit
A	$(100 \cdot 10^{-6})^2$	$1 \cdot 10^{-8}$	m ²
P	$(100 \cdot 10^{-6}) \cdot 4$	0.0004	m
D	$\frac{4 \cdot 10^{-8}}{0.0004}$	0.0001	m
Q	$\frac{250 [\mu\text{L}/\text{min}] \cdot 10^{-9}}{60}$	$4.167 \cdot 10^{-9}$	m ³ /sec
η for water	[5.1.2.3]	0.00089	Pa*s
density for water	[5.1.2.4]	998	kg/m ³
ν	$\frac{0.00089}{998}$	$8.91784 \cdot 10^{-7}$	$\frac{\text{Pa} \cdot \text{s} \cdot \text{m}^3}{\text{kg}}$
Re	$\frac{4.167 \cdot 10^{-9} \cdot 0.0001}{8.91784 \cdot 10^{-7} \cdot 10^{-8}}$	46.72	

The same calculations can be made for the other type of platforms. None crosses the laminar border of approximately 2300.



6.1.2 Mask design 1



6.1.3 Preparation progress for all wafers (1-12):

	Process	Parameters	Time
1	HMDS coating	Standard run	≈ 30 min
2	Spin-on photo resist	0 RPM	4 sec
		500 RPM	5 sec
		4000 RPM	30 sec
3	Prebake	90°C	60 sec
4	Lithography	Soft contact	3 sec
5	Development	22°C	60 sec



6.2.2 ARcare® 7815 Clear Polyester Film



PRODUCT DESCRIPTION

ARcare® 7815 is a clear, thin and flexible plastic film coated on one side with a medical grade pressure-sensitive adhesive. The adhesive side of the tape is protected by a clear siliconized polyester release liner.

FEATURES

- Non-migratory acrylic adhesive
- Inert acrylic adhesive
- Flexible adhesive system
- Easily die cut
- Tolerant to Gamma sterilization

BENEFITS

- Allows lateral flow in membrane- based devices
- Compatible with many assays
- Excellent conformability
- Facilitates design options
- Suitable for sterilization processes

PRODUCT PROFILE

Substrate: 2 mil clear polyester film
Adhesive: AS-110 acrylic medical grade adhesive
Liner: 2 mil clear siliconized polyester release film

PROPERTIES

<u>ATTRIBUTE</u>	<u>NOMINAL VALUE*</u>
180° Peel Adhesion:	40 oz/in. minimum
Optical Properties:	95.9% Light Transmission
Coat Weight:	0.95 oz./yd. ²
Thickness Without Liners:	3.0 mils
Total Thickness:	5.0 mils

*All stated values are nominal and should only be used as a guide for selection.

PRODUCT APPLICATIONS

This product is suggested for bonding, laminating and assembly of in-vitro diagnostic and related membrane-based immunoassay products. It is necessary, as with all pressure-sensitive tapes, that the surface to which the tape is to be applied be clean and dry.

SAFETY DATA

AS-110 is an acrylic, pressure-sensitive adhesive. The adhesive passed cytotoxicity and primary skin irritation tests conducted by an independent laboratory. Additional safety information is available by accessing our Drug Master Files or Device Master Files.



Product Information

ARcare® 7815

Clear Polyester Film



STORAGE

Unconverted rolls should be stored at 70° F (21° C) and 50% relative humidity, out of direct sunlight.

PRODUCT PROFILE AND DIAGRAM



(MEDPI – 06/27/05)

STORAGE OF PRESSURE-SENSITIVE ADHESIVE TAPES

Pressure-sensitive adhesive tapes function as a mechanical product; however, the adhesive itself is a chemical composition that can be sensitive to environmental conditions. A purchaser of pressure-sensitive adhesive products should be aware of the shelf life of each product and not purchase more than it can use before the expiration date. Shipping and storage conditions affect shelf life. The optimum storage temperature is 70°F (21°C). Cool, dry storage is recommended.

For best results...

- 1) The surfaces you wish to bond should be clean and free of oil, moisture and dust. If the surface temperature is below 40°F, it may be difficult to achieve a proper bond.
- 2) Do not use a pressure-sensitive adhesive product where it will be exposed to temperatures lower or higher than those designated for each product. Heat can destroy the effectiveness of the bond and extreme cold can cause the adhesive to harden and not adhere properly.
- 3) When the tape is applied, use firm hand or lamination pressure to achieve contact between the adhesive and the surface to which it is applied. Hand rollers or nip rollers may be needed for certain products or applications. Consult your AR sales representative if you need additional information.

DISCLAIMER

AR expressly warrants to Purchaser that its product, under normal and intended use maintenance and storage, is free from defects in workmanship for twelve (12) months from the date of shipment, unless otherwise stated. THIS WARRANTY IS GIVEN IN LIEU OF ALL OTHER WARRANTIES. AR MAKES NO WARRANTY AS TO EXPERIMENTAL AND DEVELOPMENTAL SAMPLES OR MATERIALS. AR MAKES NO WARRANTY OF MERCHANTABILITY OR FITNESS FOR A PARTICULAR PURPOSE. No provisions, representations, diagrams, drawings or pictures contained in any product literature, price list, catalogue, purchase order, product data sheet, order acknowledgment, invoice, delivery ticket, or any other communication by AR, including information on AR's website or representations made by AR's employees or agents, constitute express warranties. Results of tests and recommendations included in communications of AR do not constitute express warranties. SINCE MANY FACTORS MAY AFFECT THE USE AND PERFORMANCE OF AN AR PRODUCT IN A PARTICULAR APPLICATION, INCLUDING, AMONG OTHERS, THE PRODUCT SELECTED FOR USE, THE CONDITIONS IN WHICH THE PRODUCT IS USED, THE TIME AND ENVIRONMENTAL CONDITIONS IN WHICH THE PRODUCT IS EXPECTED TO PERFORM, THE MATERIALS TO BE USED WITH THE PRODUCT, THE SURFACE PREPARATION OF THOSE MATERIALS, AND THE APPLICATION METHOD FOR THE PRODUCT, PURCHASER ACCEPTS RESPONSIBILITY FOR DETERMINING WHETHER AR'S PRODUCT IS FIT FOR A PARTICULAR PURPOSE AND SUITABLE FOR PURCHASER'S METHOD OF APPLICATION. AR retains the right to modify or change its products if in AR's judgment it is advisable.

Purchaser's exclusive remedy and AR's sole obligation for any breach of warranty is limited to, at AR's option, either: 1) replacement of AR's product, or 2) reimbursement of the purchase price of AR's product. AR DISCLAIMS ANY OTHER OBLIGATION OR LIABILITIES ARISING OUT OF BREACH OF WARRANTY. AR will not be liable of any loss, damage, expense or consequential, incidental or special damages of any kind.

ARcare® and ARflow® are registered trademarks of Adhesives Research. ARseal™ is a trademark of Adhesives Research and registration is pending. Insight® is a registered service mark of Adhesives Research, Inc. Insight® - Without it, ideas languish... With it, products launch.™ is a service mark of Adhesives Research, Inc. Adhesives Research® is a registered trademark of Adhesives Research, Inc. for engineering and design services in the field of pressure-sensitive adhesive systems.
©2008 Adhesives Research, Inc. Printed in USA.

Internet: www.adhesivesresearch.com

Adhesives Research, Inc.
400 Seaks Run Road, P.O. Box 100
Glen Rock, PA 17327
Toll-free: 800-445-8240
Phone: 717-235-7979
Fax: 717-235-8320

Adhesives Research Ireland Ltd.
Raheen Business Park, Limerick, Ireland
Phone: +353 61 300 300
Fax: +353 61 300 700

Adhesives Research Ltd.
The Old Exchange, Mill Lane
Great Dunmow, Essex, UK CM8 1BG
Phone: +44 (0)1371 856300
Fax: +44 (0)1371 856380

Adhesives Research Pte. Ltd.
20 Maxwell Road
#12-08B Maxwell House
Singapore 069113
Phone: +65 6774 9580
Fax: +65 6777 7261

Adhesives Research Shanghai
Representative Office
Suite 3908, Plaza 66 Tower 1
1266 Nanjing West Road
Shanghai, China 200040
Phone: +86 21 61038526
Fax: +86 21 61038527

Adhesives Research GmbH
Stefan-George-Ring 29, D-81929
München, Germany
Phone: +49 (0) 89 930 80 220
Fax: +49 (0) 89 930 51 84

